

Mixed-state Phases from Higher-order SSPTs with Kramers-Wannier Symmetry

Aswin Parayil Mana,^{1,2} Zijian Song (宋子健),^{1,2} Fei Yan,³ and Tzu-Chieh Wei (魏子傑)^{1,2}

¹*C. N. Yang Institute for Theoretical Physics, State University of New York at Stony Brook, New York 11794, USA*

²*Department of Physics and Astronomy, State University of New York at Stony Brook, New York 11794, USA*

³*Condensed Matter Physics and Materials Science Division,*

Brookhaven National Laboratory, Upton, New York 11973, USA

(Dated: March 5, 2026)

Mixed-state phases have recently attracted significant attention as a generalization beyond their pure-state counterparts. Prominent examples include mixed-state symmetry-protected topological (mSPT) phases and the strong-to-weak symmetry breaking (SWSSB) phases. It has been shown recently that mSPT phases admit a holographic dual description in terms of higher-order subsystem SPT phases. In this work, we investigate the mixed-state phases obtained by tracing out the bulk degrees of freedom of higher-order subsystem SPT phases protected by non-invertible symmetries. We find that the resulting mixed states exhibit the coexistence of the symmetry-protected topological order and SWSSB. We also use the interface as a probe to characterize the mixed state phases, and specifically, when there is no local modification to preserve the symmetries across the interface, the two sides of the interface are in distinct phases.

Contents

I. Introduction	2	d. Tracing the interface between 2D trivial state and 2D cluster state on a cylinder with generic open boundary condition	16
II. Review of the holographic picture for mSPT phases	3	2. Mixed state from 2D blue state	16
III. Toy model of DASPTs	4	a. 2D blue state on a torus	16
A. Overview of the 2D cluster state	5	b. 2D blue state on a semi-infinite cylinder with generic boundary condition	17
B. 1D DASPT from 2D cluster state	5	c. Tracing the interface between 2D cluster state and 2D blue state on a torus	17
IV. DASPTs from non-invertible SSPTs	6	d. Tracing the interface between 2D cluster state and 2D blue state on a cylinder with generic open boundary condition	17
A. Overview of 2D blue state	7	3. Mixed state from 2D blue ^{k₀;k₁} state	17
B. 1D DASPT from 2D blue state	7	a. 2D blue ^{k₀;k₁} state on a torus	18
C. 1D DASPT from 2D blue ^{k₀;k₁} state	8	b. 2D blue ^{k₀;k₁} on a semi-infinite cylinder with generic boundary condition	18
V. Interfaces between different phases	9	c. Tracing the interface between 2D cluster state and 2D blue ^{k₀;k₁} state on a torus	18
A. Interface between trivial and $\rho_{1D-DASPT}^A$ states: different phases w.r.t. invertible symmetries	9	d. Tracing the interface between 2D cluster state and 2D blue ^{k₀;k₁} state on a cylinder with generic open boundary condition	19
B. Interface between $\rho_{1D-DASPT}^A$ and ρ_{blue}^A states: same phase w.r.t. invertible symmetries	9	B. A symmetric interface between two DASPTs	20
C. Interface between $\rho_{1D-DASPT}^A$ and $\rho_{blue^{k_0;k_1}}^A$ states: same phase w.r.t invertible symmetries	11	C. Details on the strong symmetry of ρ_{blue}^A	22
VI. Conclusion	11	D. Other choices of interface cuts	23
References	12	1. Other choices of interface cuts between $\rho_{trivial}$ and $\rho_{1D-DASPT}$	23
A. Extra examples	14	a. Interface cut at (l, k_0) and (L_x, k_0)	23
1. Mixed state from 2D cluster state	14	b. Interface cut at $(l + \frac{1}{2}, k_0 + \frac{1}{2})$ and (L_x, k_0)	23
a. 2D cluster state on a torus	14	2. Other choices of interface cuts between $\rho_{1D-DASPT}$ and ρ_{blue}	23
b. 2D cluster state on a semi-infinite cylinder with generic boundary condition	15	a. Interface cut at (l, k_0) and (L_x, k_0)	23
c. Tracing the interface between 2D trivial state and 2D cluster state on a torus	16	b. Interface cut at $(l + \frac{1}{2}, k_0 + \frac{1}{2})$ and (L_x, k_0)	24
		3. Other choices of interface cuts between $\rho_{1D-DASPT}$ and $\rho_{blue^{k_0;k_1}}$	24
		a. Interface cut at (l, k_0) and (L_x, k_0)	24
		b. Interface cut at $(l + \frac{1}{2}, k_0 + \frac{1}{2})$ and (L_x, k_0)	25

E. Commutative diagram	25
F. Some examples of 1D mixed state phases via decohering pure states (with \mathbb{Z}_2 degrees of freedom)	26
1. Example: 1D SWSSB by decohering the GHZ state	26
2. Example: 1D ASPT from decohering the cluster state in the Z basis	27
3. Example: Coexistence of SWSSB and ASPT (i.e., DASPT) by decohering the cluster state in the X basis	27
4. Example: Another DASPT by decohering the cluster state with nearest neighbor YY	28
G. 1D examples of mixed state phases and non-invertible SWSSB	28
H. 1D $\mathbb{Z}_3^{(s)} \times \mathbb{Z}_3^{(w)}$ ASPT: two ASPTs and the interface between them	30
1. ASPTs from decohering pure state SPTs	30
2. Interface between the two $\mathbb{Z}_3^{(s)} \times \mathbb{Z}_3^{(w)}$ ASPTs	31

I. Introduction

Symmetry-protected topological (SPT) phases have been extensively studied in the context of pure quantum states, with several foundational works establishing their defining properties and classification schemes [1–5]. In this framework, SPT phases are equivalence classes of gapped Hamiltonians with a fixed symmetry, where two Hamiltonians belong to the same phase if they can be connected by a symmetry-preserving adiabatic path without closing the energy gap. Equivalently, at the level of quantum states, two SPT states are in the same phase if they are related by a symmetry-respecting finite-depth local unitary (FDLU) circuit. However, any SPT state can be mapped to a trivial product state by a non-symmetric FDLU.

Extending the notion of symmetry-protected topological phases to open quantum systems remains an open challenge. In such systems, unavoidable environmental couplings and thermal fluctuations generically drive the system into mixed states, invalidating many of the assumptions underlying the pure-state classification. Recently, significant progress has been made towards extending symmetry-based classifications beyond strong symmetries, which are originally defined as symmetries of the ground state, to weak symmetries, which are symmetries of the density matrix characterizing the mixed-state system. In particular, extensive efforts have focused on strong-to-weak symmetry breaking (SWSSB) phases, mixed-state symmetry-protected topological (mSPT) phases which are also known as averaged symmetry-protected topological (ASPT) phases [6], and finite-temperature topological phases [7–46].

At finite temperature, previous works have also shown that SPT phases can persist in certain scenarios, including in three-dimensional systems protected by higher-form symmetries [47] and in two-dimensional fermionic systems [48]. Going beyond thermal states, mixed states also arise from decoherence, dissipation, as well as tracing over part of the system. Recent proposals include defining mixed-state phases via symmetric finite-depth local quantum channels [8, 9], as well as an alternative approach based on finite Markov length under local Lindbladian evolution [35]. Although each framework captures aspects of phase stability in dissipative settings, they are not equivalent. However, unlike in the pure-state case, a universally accepted definition and classification of mSPT phases remains elusive.

Non-invertible symmetries have recently attracted significant attention in both condensed matter and high-energy theory. A growing body of work has extended the notion of SPT phases to lattice systems with non-invertible symmetries, uncovering novel classes of topological phases that have no counterparts in the conventional group-symmetry setting [49–62]. As a representative example, Ref. [50] studied lattice realizations of $\text{Rep}(D_8)$ SPT phases in 1+1 dimensions, where the symmetry category includes both a $\mathbb{Z}_2 \times \mathbb{Z}_2$ symmetry and the Kramers-Wannier (KW) duality, denoted by $D^{(1)}$. In this setting, the $\mathbb{Z}_2 \times \mathbb{Z}_2$ cluster state, which is invariant under $D^{(1)}$, was shown to split into three distinct non-invertible SPT phases. Extensions to 2+1 dimensions were explored in Ref. [63], where a 2D (we omit the +1 in 2+1 for simplicity) cluster state invariant under a two-dimensional KW duality that gauges subsystem symmetries was analyzed. Owing to the presence of subsystem symmetries, this system supports a large family of SPT phases protected by non-invertible symmetries. Notably, certain subsets of these phases, when separated by a rectangular interface, differ by the presence of corner modes, thereby realizing higher-order subsystem SPT phases protected by non-invertible symmetry.

Recently, Ref. [32] investigated mixed-state SPT phases from a holographic perspective. Starting from a higher-order SPT in $(d+1)$ dimensions with subsystem symmetry \mathcal{S} and global symmetry \mathcal{G} , tracing out the bulk degrees of freedom yields a mSPT in d dimensions that exhibits a strong \mathcal{S} symmetry (supported on the boundary) and a weak \mathcal{G} symmetry. In this construction, a higher-order subsystem SPT in $(d+1)$ dimensions is holographically dual to a mSPT in d dimensions. The higher-codimensional boundary modes originate from a mixed 't Hooft anomaly between the global \mathcal{G} symmetry and the subsystem \mathcal{S} symmetry in the parent theory. This anomaly descends to the boundary, giving rise to protected boundary modes in the mSPT and manifesting as a mixed 't Hooft anomaly between the weak \mathcal{G} symmetry and the strong \mathcal{S} symmetry.

In this manuscript, we study the holographic dual description of higher-order SSPTs protected by non-invertible symmetries. By tracing out the bulk degrees of

freedom, we obtain a class of mixed-state phases. In contrast to Ref. [32], the resulting mixed state here exhibits the coexistence of both an SPT order and a strong-to-weak symmetry-breaking (SSB) structure. We refer to this phase as a doubled average SPT (DASPT) [64, 65], reflecting the presence of two extremal points characterizing the mixed-state phase. This observation does not contradict Ref. [32], since the SSPTs considered in the present work are not higher-order with respect to invertible symmetries. Instead, their higher-order nature originates from the underlying non-invertible symmetry. In terms of invertible symmetries, they belong to the same phase.

The rest of the sections are organized in the following way. In Section II, we review the holographic duality between higher-order SSPT and mSPT given in [32] using an example. In Section III, we study DASPTs by tracing out the bulk of 2D cluster state. Further in Section IV, we study the DASPTs obtained from tracing out the bulk of 2D higher-order SSPTs protected by the non-invertible Kramers-Wannier (KW) symmetry. An analysis of the interface between two different DASPTs obtained in Sections III and IV is presented in Section V. In Section VI, we provide concluding remarks and future directions. We supply further materials in the Appendices.

II. Review of the holographic picture for mSPT phases

In this section, we review the holographic picture of mSPTs, also referred to as ASPT phases [32], in more detail than previously outlined in the Introduction. A mixed-state density matrix ρ can be interpreted as the reduced density matrix of a pure state obtained by tracing out ancillary degrees of freedom. Within the holographic framework, the pure state associated with a d -dimensional mSPT is taken to be a $(d+1)$ -dimensional subsystem symmetry-protected topological (SSPT) state. Under this construction, weak symmetries of the mSPT are promoted to global symmetries of the pure-state SSPT, while strong symmetries of the mSPT become subsystem symmetries of the SSPT. Consequently, the holographic dual of a mSPT with strong \mathcal{S} symmetry and weak \mathcal{G} symmetry is a higher-order SSPT

characterized by subsystem \mathcal{S} symmetry and global \mathcal{G} symmetry. The SSPT wave function exhibits short-range correlations in both the bulk and side surfaces, while hosting gapless modes localized at the hinges. These hinge modes realize a mixed anomaly between the global symmetry \mathcal{G} and the subsystem symmetry \mathcal{S} . This observation suggests that the reduced density matrix of the two-dimensional SSPT wave function effectively behaves as a one-dimensional mSPT, motivating the following duality:

$$\begin{array}{c} \text{SSPT wavefunction in } d+1 \text{ dim} \\ \updownarrow \\ \text{mSPT in } d \text{ dim.} \end{array}$$

These mSPTs can be probed using the fidelity strange correlator. Let $\rho = |\Psi_{\text{SSPT}}\rangle\langle\Psi_{\text{SSPT}}|$ and $\rho_0 = |\Psi_0\rangle\langle\Psi_0|$, where $|\Psi_0\rangle$ is a trivial product state. By tracing out ancillary degrees of freedom, we obtain one-dimensional mSPTs $\xi[\rho]$ and $\xi[\rho_0]$. These states can be distinguished through the fidelity strange correlator

$$\frac{F(\xi[\rho], O_r O_{r'}^\dagger \xi[\rho_0] O_{r'} O_r^\dagger)}{F(\xi[\rho], \xi[\rho_0])},$$

which exhibits power-law decay as a function of $|r-r'|$. Here, ξ denotes the decoherence channel that prepares the mSPT from the SSPT wave function, and \mathcal{O} is an operator charged under the strong symmetry \mathcal{S} . As shown in Ref. [32], this fidelity strange correlator is lower bounded by the strange correlator computed directly from the SSPT wave function and the product state $|\Psi_0\rangle$.

We now illustrate the holographic duality between SSPT phases and mSPTs using an explicit example introduced in Ref. [32]. Consider a two-dimensional lattice composed of two sets of spin chains oriented along the x -direction at each fixed value of y , which we label as the left (L) and right (R) chains. Along each row and at a given x -coordinate, there are two spins denoted by σ and τ . Consequently, each unit cell at position (x,y) contains four spins: $\sigma_L, \tau_L, \sigma_R,$ and τ_R . See Figure 1 for an illustration.

We consider the following Hamiltonian,

$$\begin{aligned} \text{H} = & - \sum_{\alpha=L,R} [\sigma_\alpha^z(x,y)\tau_\alpha^x(x,y)\sigma_\alpha^z(x+1,y) + J\sigma_L^z(x,y)\sigma_R^z(x,y+1) \\ & + \tau_L^z(x,y)\sigma_L^x(x+1,y)\tau_L^z(x+1,y)\tau_R^z(x,y+1)\sigma_R^x(x+1,y+1)\tau_R^z(x+1,y+1)] \end{aligned} \quad (1)$$

This Hamiltonian possesses subsystem symmetries acting

independently along each x -row,

$$U_s^R(y) = \prod_x \tau_R^x(x,y), \quad U_s^L(y) = \prod_x \tau_L^x(x,y). \quad (2)$$

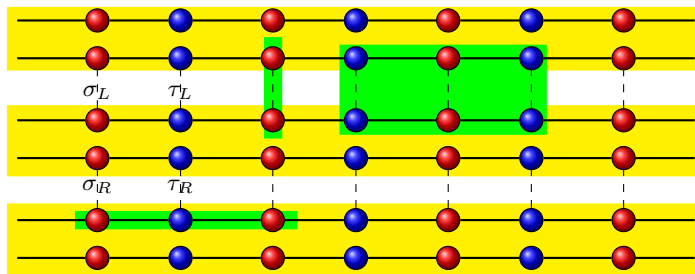


FIG. 1: Arrangement of qubits for the 2D SSPT Hamiltonian in (1). Each unit cell contains two types (L and R) of σ and τ spins. The green regions specify the different interactions in the SSPT Hamiltonian (1). Each yellow region contains two L and R spin chains.

as well as a global \mathbb{Z}_2 symmetry given by

$$U_g = \prod_{x,y} \sigma_L^x(x,y) \sigma_R^x(x,y). \quad (3)$$

In the presence of an open, smooth boundary at $x = 0$, each y -row along the edge hosts two sets of dangling spin- $\frac{1}{2}$ degrees of freedom, labeled by L and R . These spins can be paired into on-site singlets that are invariant under both the subsystem $\mathbb{Z}_2 \times \mathbb{Z}_2$ symmetry and the global \mathbb{Z}_2 symmetry, thereby fully gapping the edge.

For a system with open boundaries at both $x = 0$ and $y = 0$, the edge at $y = 0$ contains an R -spin chain that is decoupled from the bulk building blocks. One may introduce edge transverse-field terms τ_R^x and σ_R^x along $y = 0$, which gap out this R -spin chain without breaking any symmetries. However, at the corner $x = y = 0$, where the two edges intersect, there remain residual Pauli operators \tilde{X}_L , \tilde{Y}_L , and \tilde{Z}_L that are decoupled from both the bulk and the gapped edges. These remaining spin- $\frac{1}{2}$ degrees of freedom transform projectively under the combined action of the subsystem $\mathbb{Z}_2 \times \mathbb{Z}_2$ symmetry and the global \mathbb{Z}_2 symmetry, giving rise to a protected corner mode.

We now impose periodic boundary conditions and trace out all spin chains except for a single one. The resulting reduced density matrix takes the form

$$\rho = \frac{1}{2^N} \sum_{\{\mathcal{D}\}} |\Psi_{\mathcal{D}}\rangle \langle \Psi_{\mathcal{D}}|, \quad (4)$$

where N denotes the number of sites along the x -direction, and the sum runs over all configurations $\{\mathcal{D}\}$. The pure states $|\Psi_{\mathcal{D}}\rangle$ are given by

$$|\Psi_{\mathcal{D}}\rangle = \bigotimes_j |\sigma_j^z = h_j\rangle \otimes |\tau_j^x = h_j h_{j+1}\rangle, \quad (5)$$

with $h_j = \pm 1$ labeling classical d.o.f., and σ and τ are the remaining d.o.f. in the one-dimensional boundary.

The reduced density matrix ρ is invariant under a strong \mathbb{Z}_2 symmetry,

$$U_s = \prod_j \tau_j^x, \quad (6)$$

which originates from a subsystem symmetry inherited from the parent SSPT, as well as a weak \mathbb{Z}_2 symmetry,

$$U_g = \prod_j \sigma_j^x. \quad (7)$$

The state ρ exhibits a nonvanishing, constant fidelity strange correlator with a trivial product state when evaluated using the charged operator $O = \tau^z$ associated with the strong symmetry, indicating ρ is a non-trivial mSPT.

In the remaining sections, we will focus on examples of higher-order SSPTs with non-invertible symmetries. When only invertible symmetries are present, the phases we consider below are SSPTs but not higher-order SSPTs. Tracing out the bulk, the subsystem symmetries on the boundary become the strong global symmetry for the mixed state. However, the resulting mixed state is not solely an SPT but exhibits the coexistence of SPT and SWSSB, namely the DASPT. We emphasize that a 2D non-invertible symmetry does not necessarily give rise to a 1D non-invertible symmetry upon tracing out the bulk. Starting from different 2D non-invertible SPT states, one may in some cases observe the emergence of a 1D non-invertible symmetry after tracing out the bulk, while in other cases no such symmetry appears. Below, we analyze these distinct scenarios in more detail.

III. Toy model of DASPTs

In this section, we study a simple example of 1D DASPT obtained by placing the 2D cluster state on a semi-infinite cylinder with Dirichlet boundary condition and tracing out the bulk degrees of freedom. We refer the reader to Appendix F for other examples of 1D mixed state phases involving invertible symmetries obtained by decohering various pure states, which serves as an alternative method to obtain mixed state phases. See also Appendix G for an example of SWSSB of non-invertible symmetry. In Appendix E, we present a commutative diagram illustrating the relationship between tracing and decoherence in obtaining 1D mixed states from 2D pure states.

A. Overview of the 2D cluster state

Consider two mutually dual two-dimensional square lattices, as illustrated in Figure 2, distinguished by red and blue coloring, with degrees of freedom residing on their vertices. We denote the vertices and plaquettes of the red lattice by v_r and p_r , and those of the blue lattice by v_b and p_b , respectively. We identify p_b with v_r and p_r with v_b . There are L_x vertices along the x -direction and L_y vertices along the y -direction. Vertices of the red sublattice are labeled by integer coordinates (i, j) , whereas vertices of the blue sublattice are labeled by half-integer coordinates $(i + \frac{1}{2}, j + \frac{1}{2})$, where $i = 1, \dots, L_x$ and $j = 1, \dots, L_y$. We denote the sets of vertices and plaquettes on the red and blue sublattices by Δ_{v_r} , Δ_{p_r} , Δ_{v_b} , and Δ_{p_b} , respectively. We use ∂p to denote the vertices around the plaquette p . The corresponding cluster Hamiltonian is given by

$$H_{2D\text{-cluster}} = - \sum_{v_r} X_{v_r} \prod_{v_b \in \partial p_b} Z_{v_b} - \sum_{v_b} X_{v_b} \prod_{v_r \in \partial p_r} Z_{v_r}. \quad (8)$$

The ground state of this Hamiltonian is the cluster state

$$|2D\text{-cluster}\rangle = \prod_{p_b=v_r \in \Delta_{v_r}} \prod_{v_b \in \partial p_b} CZ_{v_r, v_b} |+\rangle^{\otimes \Delta_{v_r}} |+\rangle^{\otimes \Delta_{v_b}}, \quad (9)$$

where $|+\rangle^{\otimes \Delta_{v_r}}$ and $|+\rangle^{\otimes \Delta_{v_b}}$ denote, respectively, the tensor product of $|+\rangle$ states over all vertex degrees of freedom associated with each of the two sublattices.

The cluster Hamiltonian (8) possesses subsystem symmetries generated by

$$\begin{aligned} \eta_{r,j}^x &= \prod_i X_{i,j}, & \eta_{r,i}^y &= \prod_j X_{i,j}, \\ \eta_{b,j}^x &= \prod_i X_{i+\frac{1}{2}, j+\frac{1}{2}}, & \eta_{b,i}^y &= \prod_j X_{i+\frac{1}{2}, j+\frac{1}{2}}. \end{aligned} \quad (10)$$

In addition to these symmetries, there is another symmetry for the Hamiltonian in Eq. (8) obtained by swapping the following terms,

$$X_{v_r} \leftrightarrow \frac{Z_{v_b}}{Z_{v_b}} \frac{Z_{v_b}}{Z_{v_b}}, \quad X_{v_b} \leftrightarrow \frac{Z_{v_r}}{Z_{v_r}} \frac{Z_{v_r}}{Z_{v_r}}. \quad (11)$$

This transformation is the same as that of Kramers-Wannier duality which is obtained by gauging the subsystem symmetries. An operator representation of this symmetry up to a half lattice translation is given in [66]. Here we define an operator with half lattice translation included:

$$\mathbf{D}^{(2)} = \mathbf{T}_{\frac{1}{2}, \frac{1}{2}}^{-1} \mathbf{D}_r^{(2)} \mathbf{D}_b^{(2)}. \quad (12)$$

The operator $\mathbf{D}_{r(b)}^{(2)}$ on the red(blue) sublattice is defined as

$$\mathbf{D}_{r(b)}^{(2)} \equiv \mathbf{P}_{r(b)}^{(2)} \tilde{\mathbf{D}}_{x;r(b)}^{(2)} \mathbf{H}_{r(b)}^{\otimes(2)} \tilde{\mathbf{D}}_{y;r(b)}^{(2)} \mathbf{P}_{r(b)}^{(2)}, \quad (13)$$

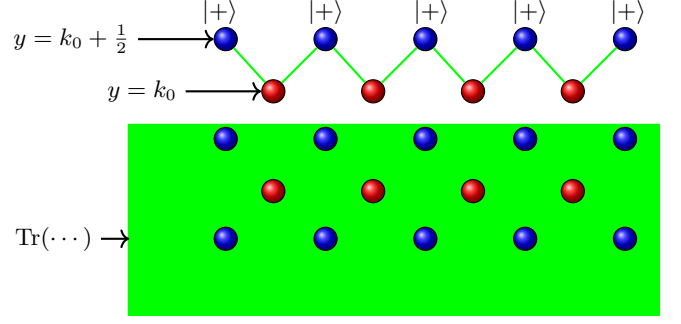


FIG. 2: Bipartite lattice with open boundary condition in the y direction and periodic boundary condition in the x direction. The top boundary is at $y = k_0 + \frac{1}{2}$. We trace out all the d.o.f. except those on region A defined to be the rows at $y = k_0$ and $y = k_0 + \frac{1}{2}$. Green region contains the d.o.f. that we trace over. One can set the boundary row reference k_0 to zero without loss of generality.

where $\mathbf{H}_{r(b)}^{\otimes(2)}$ denotes the product of Hadamard operators on red (or blue) lattice and

$$\tilde{\mathbf{D}}_{x;r}^{(2)} \equiv \prod_{j=1}^{L_y} \left(\left(\prod_{i=1}^{L_x-1} e^{i\frac{\pi}{4} X_{i,j}} e^{i\frac{\pi}{4} Z_{i,j} Z_{i+1,j}} \right) e^{i\frac{\pi}{4} X_{L_x,j}} \right), \quad (14a)$$

$$\tilde{\mathbf{D}}_{y;r}^{(2)} \equiv \prod_{i=1}^{L_x} \left(\left(\prod_{j=1}^{L_y-1} e^{i\frac{\pi}{4} X_{i,j}} e^{i\frac{\pi}{4} Z_{i,j} Z_{i,j+1}} \right) e^{i\frac{\pi}{4} X_{i,L_y}} \right), \quad (14b)$$

$$\mathbf{P}_r^{(2)} \equiv \prod_{j=1}^{L_y} \frac{(1 + \eta_{r,j}^x)}{2} \prod_{i=1}^{L_x} \frac{(1 + \eta_{r,i}^y)}{2}, \quad (14c)$$

with similar definitions for $\tilde{\mathbf{D}}_{x;b}^{(2)}$, $\tilde{\mathbf{D}}_{y;b}^{(2)}$ and $\mathbf{P}_b^{(2)}$.

The symmetry operator $\mathbf{D}^{(2)}$ is non-invertible and satisfies the following fusion rules

$$\begin{aligned} (\mathbf{D}^{(2)})^2 &\propto \mathbf{P}_r^{(2)} \mathbf{P}_b^{(2)}, \\ \eta_{r,j}^x \mathbf{D}^{(2)} &= \mathbf{D}^{(2)} \eta_{r,j}^x = \mathbf{D}^{(2)}, \\ \eta_{r,i}^y \mathbf{D}^{(2)} &= \mathbf{D}^{(2)} \eta_{r,i}^y = \mathbf{D}^{(2)}, \\ \eta_{b,j+\frac{1}{2}}^x \mathbf{D}^{(2)} &= \mathbf{D}^{(2)} \eta_{b,j+\frac{1}{2}}^x = \mathbf{D}^{(2)}, \\ \eta_{b,i+\frac{1}{2}}^y \mathbf{D}^{(2)} &= \mathbf{D}^{(2)} \eta_{b,i+\frac{1}{2}}^y = \mathbf{D}^{(2)}. \end{aligned} \quad (15)$$

B. 1D DASPT from 2D cluster state

We now place the 2d cluster state on a semi-infinite cylinder, whose open boundary along the y -direction consists of the row of blue vertices at $y = k_0 + \frac{1}{2}$ and the

row of red vertices at $y = k_0$, as illustrated in Figure 2. Moreover, we consider a Dirichlet-type boundary condition where all the vertices in the row of blue vertices are in the $|+\rangle$ state. See Appendix A 1 for other choices of boundary conditions.

Tracing out the bulk gives the following mixed state

$$\rho_{\text{1D-DASPT}}^{\text{A}} = \prod_i \left(\frac{1 + Z_{i,k_0} X_{i+\frac{1}{2},k_0+\frac{1}{2}} Z_{i+1,k_0}}{2} \right) \times \frac{(1 + \prod_i X_{i,k_0})}{2^{|\Delta_{v_r} \cap \text{A}|}}. \quad (16)$$

The superscript A indicates the remaining sites after tracing over the rest. This state has two strong symmetries: $\mathbb{Z}_2^{(r)} = \prod_i X_{i,k_0}$ and $\mathbb{Z}_2^{(b)} = \prod_i X_{i+\frac{1}{2},k_0+\frac{1}{2}}$.

The two sets of stabilizers inherited from the 2D cluster state, $Z_{i,k_0} X_{i+\frac{1}{2},k_0+\frac{1}{2}} Z_{i+1,k_0}$ and $Z_{i-\frac{1}{2},k_0+\frac{1}{2}} X_{i,k_0} Z_{i+\frac{1}{2},k_0+\frac{1}{2}}$, act differently on the mixed state $\rho_{\text{1D-DASPT}}^{\text{A}}$. One set of stabilizer satisfies a strong symmetry condition while the other set satisfies a weak symmetry condition. Concretely we have

$$Z_{i,k_0} X_{i+\frac{1}{2},k_0+\frac{1}{2}} Z_{i+1,k_0} \rho_{\text{1D-DASPT}}^{\text{A}} = \rho_{\text{1D-DASPT}}^{\text{A}}, \quad (17a)$$

$$Z_{i-\frac{1}{2},k_0+\frac{1}{2}} X_{i,k_0} Z_{i+\frac{1}{2},k_0+\frac{1}{2}} \rho_{\text{1D-DASPT}}^{\text{A}} Z_{i-\frac{1}{2},k_0+\frac{1}{2}} X_{i,k_0} Z_{i+\frac{1}{2},k_0+\frac{1}{2}} = \rho_{\text{1D-DASPT}}^{\text{A}}. \quad (17b)$$

We note that this state can also be obtained by decohering the pure 1D cluster state, whose density matrix is

$$\rho_{\text{pSPT}} = \prod_i \left(\frac{1 + Z_{i,k_0} X_{i+\frac{1}{2},k_0+\frac{1}{2}} Z_{i+1,k_0}}{2} \right) \prod_i \left(\frac{1 + Z_{i-\frac{1}{2},k_0+\frac{1}{2}} X_{i,k_0} Z_{i+\frac{1}{2},k_0+\frac{1}{2}}}{2} \right), \quad (18)$$

with decoherence channel

$$\xi[\rho_{\text{pSPT}}] = \prod_i \xi_i[\rho_{\text{pSPT}}], \quad (19)$$

where

$$\xi_i[\rho_{\text{pSPT}}] = \frac{1}{2} (\rho_{\text{pSPT}} + Z_{i,k_0} Z_{i+1,k_0} \rho_{\text{pSPT}} Z_{i,k_0} Z_{i+1,k_0}). \quad (20)$$

Using the fidelity correlator or Rényi-2 correlator defined in [23], it can be checked that $\rho_{\text{1D-DASPT}}^{\text{A}}$ is in the SWSSB phase with respect to the $\mathbb{Z}_2^{(r)}$ symmetry on the red sublattice. Namely we have

$$\text{Tr} \left(Z_{i,k_0} Z_{j,k_0} \rho_{\text{1D-DASPT}}^{\text{A}} Z_{i,k_0} Z_{j,k_0} \rho_{\text{1D-DASPT}}^{\text{A}} \right) = 1, \quad (21)$$

$$\text{Tr} \left(\sqrt{\rho_{\text{1D-DASPT}}^{\text{A}}} Z_{i,k_0} Z_{j,k_0} \rho_{\text{1D-DASPT}}^{\text{A}} Z_{i,k_0} Z_{j,k_0} \sqrt{\rho_{\text{1D-DASPT}}^{\text{A}}} \right) = 1.$$

On the other hand, consider the following string order parameter for the strong $\mathbb{Z}_2^{(b)}$ symmetry

$$\mathcal{O}_{i,l}^{(b)} := Z_{i,k_0} X_{i+\frac{1}{2},k_0+\frac{1}{2}} X_{i+\frac{3}{2},k_0+\frac{1}{2}} \cdots X_{i+l+\frac{1}{2},k_0+\frac{1}{2}} Z_{i+l+1,k_0}, \quad (22)$$

where i can be any red site in the row $y = k_0$. The expectation value of this string order parameter on $\rho_{\text{1D-DASPT}}^{\text{A}}$ is computed to be

$$\text{Tr} \left(\mathcal{O}_{i,l}^{(b)} \rho_{\text{1D-DASPT}}^{\text{A}} \right) = 1. \quad (23)$$

This implies non-trivial edge correlations as discussed in [9], as well as the standard symmetry localization at boundaries.

Therefore, we see that $\rho_{\text{1D-DASPT}}^{\text{A}}$ exhibits both properties of ASPT and SWSSB, $\rho_{\text{1D-DASPT}}^{\text{A}}$ is thus referred as a doubled average SPT (DASPT) state, which was recently numerically explored in [64, 65]. In contrast, in the mixed-state examples in Ref. [32] by tracing over the bulk, only ASPT phases emerge.

We note that existence of symmetry breaking order and SPT order appeared in the pure ground states [67, 68] and in non-equilibrium settings [69].

In addition to the invertible $\mathbb{Z}_2^{(r)}$ and $\mathbb{Z}_2^{(b)}$ symmetries discussed above, there is an emergent strong non-invertible KW symmetry [50, 66] in the one-dimensional system,

$$D^{(1)} = \mathbf{T}^{-1} D_r D_b, \quad (24)$$

where D_r and D_b are non-invertible KW symmetry operators on the red row and blue row in the region A. The exact expression for the KW symmetry operator D (this could be D_r or D_b) on a ring with L sites is given by [70–72]

$$D = \prod_{i=1}^{L-1} \left(e^{i\frac{\pi}{4} X_i} e^{i\frac{\pi}{4} Z_i Z_{i+1}} \right) e^{i\frac{\pi}{4} X_L} \times \frac{(1 + \prod_i X_{2i})}{2} \frac{(1 + \prod_i X_{2i+1})}{2}. \quad (25)$$

$D^{(1)}$ has the following action on the Pauli operators

$$X_{i,k} \xrightarrow{D^{(1)}} Z_{i-\frac{1}{2},k+\frac{1}{2}} Z_{i+\frac{1}{2},k+\frac{1}{2}}, \quad (26a)$$

$$X_{i+\frac{1}{2},k+\frac{1}{2}} \xrightarrow{D^{(1)}} Z_{i,k} Z_{i+1,k}. \quad (26b)$$

From the above action of $D^{(1)}$ together with the stabilizer condition, it follows that $D^{(1)}$ is a strong symmetry for $\rho_{\text{1D-DASPT}}^{\text{A}}$.

A summary of the features of $\rho_{\text{1D-DASPT}}^{\text{A}}$ is given in Table I and II.

IV. DASPTs from non-invertible SSPTs

In this section, we study the mixed state phase by tracing out a different SSPT state with the non-invertible

Kramers-Wannier symmetry. In particular, we first consider a non-invertible higher order SSPT studied in [63], denoted as the *blue state*. Later we will also study another state denoted as $blue^{k_0; k_1}$. Our setup is the same as illustrated in Figure 2.

We start with 2D states that are in a different phase from the 2D cluster state due to the non-invertible symmetry $\mathbf{D}^{(2)}$. These states can be obtained by considering the Kennedy-Tasaki transformation which maps SPT to SSB phases. Under KT, the non-invertible symmetry operator $\mathbf{D}^{(2)}$ is mapped to an operator proportional to $\hat{V} = \prod_{v_r, v_b} CZ_{v_r, v_b}$, while the subsystem symmetries are mapped to the subsystem symmetries on the dual theory. KT maps the cluster phase to spontaneous symmetry breaking phase that consists of two copies of plaquette Ising model. Hence, all the subsystem symmetries are spontaneously broken. However, there are various choices for the preserved symmetries. \hat{V} is one such choice and on the dual theory side this gives rise to the cluster phase protected by the non-invertible symmetry $\mathbf{D}^{(2)}$, which we already discussed in the previous section. Another choice is preserving $\hat{V} \prod_{v_r} X_{v_r}$, and this on the dual theory side gives the blue phase, which we describe below.

A. Overview of 2D blue state

The 2D blue state is in the same phase as the 2D cluster state if we only take into account the subsystem symmetries. However, including the non-invertible symmetry (12), the cluster phase splits into different phases and the blue state is in a different phase from the cluster phase protected by the non-invertible symmetry [63]. The Hamiltonian of one such refined phase due to the splitting is described by the cluster Hamiltonian itself. On the other hand, the Hamiltonian for the phase associated with the blue state is also translation invariant and is given by

$$H_{\text{blue}} = \sum_{v_r} \begin{array}{c} Z_{v_b} \\ \square \\ X_{v_r} \\ \square \\ Z_{v_b} \end{array} - \sum_{v_b} \begin{array}{c} Y_{v_r} \\ \square \\ X_{v_b} \\ \square \\ Y_{v_r} \end{array} - \sum_{v_b} \begin{array}{c} Z_{v_b} \\ \square \\ X_{v_b} \\ \square \\ Z_{v_b} \end{array} . \quad (27)$$

The two phases differ as a higher-order SSPT with protected corner modes between their interface. We note that there are additional phases that are different from the cluster phase whose corresponding Hamiltonian is not translation invariant; see [63] for a detailed analysis of such phases.

The Hamiltonian (27) has a unique ground state (which we have referred to as the blue state above) given by

$$|\text{blue}\rangle = \prod_{v_b} CZ_{v_b, v_b+(1,1)} CZ_{v_b, v_b+(-1,1)} \times \prod_{v_r} \prod_{v_b \in \partial(p_b=v_r)} CZ_{v_r, v_b} |+\rangle^{\otimes \Delta_{v_b}} |-\rangle^{\Delta_{v_r}} . \quad (28)$$

The state $|\text{blue}\rangle$ is related to the 2D cluster state $|\text{2D-cluster}\rangle$ (the ground state of (8)) by the following finite-depth circuit

$$\prod_{v_r} Z_{v_r} \prod_{v_b} CZ_{v_b, v_b+(1,1)} CZ_{v_b, v_b+(-1,1)} . \quad (29)$$

However, such a circuit does not respect the 2D KW symmetry, and, therefore, the cluster and blue states remain at different phases characterized by the KW symmetry.

B. 1D DASPT from 2D blue state

We now consider the Hamiltonian H_{blue} on a cylinder, i.e. with open boundary condition on the y direction, with the top boundary on blue vertices at $y = k_0 + \frac{1}{2}$. We consider the Dirichlet boundary condition where all the vertex d.o.f. at $k_0 + \frac{1}{2}$ is set to $|+\rangle$. The analysis for other choices of boundary conditions is shown in Appendix A 2. Now, just as illustrated in Figure 2, we trace out all the 2D d.o.f. except for region A consisting of the top rows at $y = k_0$ and $y = k_0 + \frac{1}{2}$,

$$\rho_{\text{blue}}^A \equiv \text{Tr}_{A^c} (|\text{blue}\rangle \langle \text{blue}|) = \frac{2}{2^{|\Delta_{v_r} \cap A|}} \sum_{\substack{\{i_1\} \in \Delta_{v_r} \cap A, \\ s \text{ even}}} (Z_{i_1} \prod_{j_1 \in \text{Nb}(i_1)} Z_{j_1}) \dots (Z_{i_s} \prod_{j_s \in \text{Nb}(i_s)} Z_{j_s}) \prod_{v_r, v_b} CZ_{v_r, v_b} |+\rangle^{\otimes \Delta_{v_r}} |+\rangle^{\otimes \Delta_{v_b}} \langle +|^{\otimes \Delta_{v_b}} \langle +|^{\otimes \Delta_{v_r}} \prod_{v_r, v_b} CZ_{v_r, v_b} (Z_{i_1} \prod_{j_1 \in \text{Nb}(i_1)} Z_{j_1}) \dots (Z_{i_s} \prod_{j_s \in \text{Nb}(i_s)} Z_{j_s}) \quad (30)$$

where $\text{Nb}(i_l)$ denotes the neighboring blue vertices to the red vertex i_l in A. This state has strong $\mathbb{Z}_2^{(r)} \times \mathbb{Z}_2^{(b)}$ 0-form symmetry and an emergent non-invertible symmetry $D^{(1)}$ [50, 66]. Although not obvious, the non-invertible symmetry $D^{(1)}$ is a strong symmetry for ρ_{blue}^A , and we leave the detailed calculations to Appendix C.

Additionally, we have the following strong and weak stabilizers

$$Z_{i-\frac{1}{2},k_0+\frac{1}{2}} Y_{i,k_0} X_{i+\frac{1}{2},k_0+\frac{1}{2}} Y_{i+1,k_0} Z_{i+\frac{1}{2},k_0+\frac{1}{2}} \rho_{\text{blue}}^A = -\rho_{\text{blue}}^A, \quad (31a)$$

$$\begin{aligned} Z_{i,k} X_{i+\frac{1}{2},k_0+\frac{1}{2}} Z_{i+1,k_0} \rho_{\text{blue}}^A Z_{i,k} X_{i+\frac{1}{2},k_0+\frac{1}{2}} Z_{i+1,k_0} \\ = \rho_{\text{blue}}^A, \end{aligned} \quad (31b)$$

$$\begin{aligned} Z_{i-\frac{1}{2},k_0+\frac{1}{2}} X_{i,k_0} Z_{i+\frac{1}{2},k_0+\frac{1}{2}} \rho_{\text{blue}}^A Z_{i-\frac{1}{2},k_0+\frac{1}{2}} X_{i,k_0} Z_{i+\frac{1}{2},k_0+\frac{1}{2}} \\ = \rho_{\text{blue}}^A. \end{aligned} \quad (31c)$$

From the above we infer that

$$\begin{aligned} \rho_{\text{blue}}^A = \prod_i \left(\frac{1 - Z_{i-\frac{1}{2},k_0+\frac{1}{2}} Y_{i,k_0} X_{i+\frac{1}{2},k_0+\frac{1}{2}} Y_{i+1,k_0} Z_{i+\frac{1}{2},k_0+\frac{1}{2}}}{2} \right) \\ \times \left(\frac{1 + \prod_i X_{i,k_0}}{2^{|\Delta_{v_r} \cap A|}} \right). \end{aligned} \quad (32)$$

We note that this state is also a DASPT state, but with a different form from Eq. (16). We will study their interface in VB. A summary of properties of ρ_{blue}^A is given in Table III and IV.

C. 1D DASPT from 2D blue $^{k_0;k_1}$ state

Here we consider yet another choice of SSB phase that preserves $\prod CZ_{v_r, v_b} \times \prod_{k_1 \leq j \leq k_0} \prod_i X_{v_r=(i,j)}$ and breaks all subsystem symmetries. The corresponding dual SSPT state is

$$\begin{aligned} |\text{blue}^{k_0;k_1}\rangle \\ = \prod_{\substack{v_b=(i+\frac{1}{2},j+\frac{1}{2}) \\ k_1 \leq j \leq k_0-1}} CZ_{v_b, v_b+(1,1)} CZ_{v_b, v_b+(-1,1)} \\ \times \prod_{\substack{v_b=(i+\frac{1}{2},j+\frac{1}{2}) \\ j=k_0}} CZ_{v_b, v_b+(1,0)} \prod_{\substack{v_b=(i+\frac{1}{2},j+\frac{1}{2}) \\ j=k_1-1}} CZ_{v_b, v_b+(1,0)} \\ \times \prod_{v_r} \prod_{v_b \in \partial(p_b=v_r)} CZ_{v_r, v_b} |+\rangle^{\otimes \Delta_{v_b}} |-\rangle^{\otimes \Delta_{v_r}}. \end{aligned} \quad (33)$$

Now we place the blue $^{k_0;k_1}$ state on a geometry with open boundary condition in the y direction with y values ranging from $-\infty$ to $k_1, k_1 + \frac{1}{2}, k_1 + 1, \dots, k_0 - \frac{1}{2}, k_0, k_0 + \frac{1}{2}$. We further impose the Dirichlet boundary condition where all the vertex d.o.f at $k_0 + \frac{1}{2}$ is set to $|+\rangle$. We leave the analysis to Appendix A3 for other choices of boundary conditions. Taking $y = k_0$ and $y = k_0 + \frac{1}{2}$ as the region A and the rest as A^c as before, after tracing

out the region A^c, we obtain the following mixed state

$$\begin{aligned} \text{Tr}_{A^c} \left(|\text{blue}^{k_0;k_1}\rangle \langle \text{blue}^{k_0;k_1}| \right) \\ = \left[\prod_{v_b=(i+\frac{1}{2},k_0+\frac{1}{2})} CZ_{v_b, v_b+(1,0)} \right] \rho_{\text{blue}}^A \\ \times \left[\prod_{v_b=(i+\frac{1}{2},k_0+\frac{1}{2})} CZ_{v_b, v_b+(1,0)} \right] \equiv \rho_{\text{blue}^{k_0;k_1}}^A. \end{aligned} \quad (34)$$

This state has strong $\mathbb{Z}_2^{(r)} \times \mathbb{Z}_2^{(b)}$ 0-form symmetry and no strong/weak non-invertible symmetry $D^{(1)}$. In addition, we have the strong and weak stabilizers

$$Y_{i,k_0} X_{i+\frac{1}{2},k_0+\frac{1}{2}} Y_{i+1,k_0} \rho_{\text{blue}^{k_0;k_1}}^A = -\rho_{\text{blue}^{k_0;k_1}}^A \quad (35a)$$

$$\begin{aligned} Z_{i,k_0} X_{i+\frac{1}{2},k_0+\frac{1}{2}} Z_{i+1,k_0} \rho_{\text{blue}^{k_0;k_1}}^A Z_{i,k_0} X_{i+\frac{1}{2},k_0+\frac{1}{2}} Z_{i+1,k_0} \\ = \rho_{\text{blue}^{k_0;k_1}}^A, \end{aligned} \quad (35b)$$

From the above we infer that this state can be explicitly written in terms of the following projectors

$$\begin{aligned} \rho_{\text{blue}^{k_0;k_1}}^A = \prod_i \left(\frac{1 - Y_{i,k_0} X_{i+\frac{1}{2},k_0+\frac{1}{2}} Y_{i+1,k_0}}{2} \right) \\ \times \left(\frac{1 + \prod_i X_{i,k_0}}{2^{|\Delta_{v_r} \cap A|}} \right). \end{aligned} \quad (36)$$

We note that this state is also a DASPT state different from $\rho_{\text{1D-DASPT}}^A$. However, this state has different symmetries compared to $\rho_{\text{1D-DASPT}}^A$ as the later possesses the strong non-invertible symmetry $D^{(1)}$ but the former is not symmetric under $D^{(1)}$. A summary of the properties of $\rho_{\text{blue}^{k_0;k_1}}^A$ can be found in Table V and VI.

Additionally, this state can also be obtained by decohering the following pure state 1D non-invertible SPT [50]

$$\begin{aligned} \rho_{\text{pNSPT}} = \prod_i \left(\frac{1 - Y_{i,k_0} X_{i+\frac{1}{2},k_0+\frac{1}{2}} Y_{i+1,k_0}}{2} \right) \\ \prod_i \left(\frac{1 - Z_{i-\frac{1}{2},k_0+\frac{1}{2}} X_{i,k_0} Z_{i+\frac{1}{2},k_0+\frac{1}{2}}}{2} \right), \end{aligned} \quad (37)$$

with decoherence channel

$$\xi[\rho_{\text{pNSPT}}] = \prod_i \xi_i[\rho_{\text{pNSPT}}], \quad (38)$$

where

$$\xi_i[\rho_{\text{pNSPT}}] = \frac{1}{2} (\rho_{\text{pNSPT}} + Y_{i,k_0} Y_{i+1,k_0} \rho_{\text{pNSPT}} Y_{i,k_0} Y_{i+1,k_0}). \quad (39)$$

If we take Pauli- Y operators as charged under the strong $\mathbb{Z}_2^{(r)}$ symmetry, we find the Rényi-2 correlator

$$\text{Tr} (Y_{i,k_0} Y_{j,k_0} \rho_{\text{blue}^{k_0;k_1}}^A Y_{i,k_0} Y_{j,k_0} \rho_{\text{blue}^{k_0;k_1}}^A) = 1, \quad (40)$$

and the fidelity correlator

$$\begin{aligned} \text{Tr} \left(\sqrt{\rho_{\text{blue}^{k_0;k_1}}^A} Y_{i,k_0} Y_{j,k_0} \rho_{\text{blue}^{k_0;k_1}}^A Y_{i,k_0} Y_{j,k_0} \sqrt{\rho_{\text{blue}^{k_0;k_1}}^A} \right) \\ = 1. \end{aligned} \quad (41)$$

This confirms that the strong $\mathbb{Z}_2^{(r)}$ symmetry is spontaneously broken to a weak symmetry.

V. Interfaces between different phases

In this section, we study the interface between two different ASPTs. First, we consider the interface between the trivial state and the doubled ASPT state $\rho_{\text{1D-DASPT}}^A$ obtained from tracing out the 2D cluster state. Then, we study the interface between $\rho_{\text{1D-DASPT}}^A$ and ρ_{blue}^A obtained from tracing out the 2D cluster state and 2D blue state respectively. Finally, we investigate the interface between $\rho_{\text{1D-DASPT}}^A$ and $\rho_{\text{blue}^{k_0;k_1}}^A$ obtained from tracing out the 2D cluster state and 2D blue ^{$k_0;k_1$} state respectively. In Appendix B, we provide the analysis for the interface between $\rho_{\text{1D-DASPT}}^A$ and another similar-looking DASPT. In Appendix H, we perform an interface analysis between two different mixed state SPTs protected by $\mathbb{Z}_3^{(s)} \times \mathbb{Z}_3^{(w)}$.

A. Interface between trivial and $\rho_{\text{1D-DASPT}}^A$ states: different phases w.r.t. invertible symmetries

Let us consider the interface between the 2D trivial state and the 2D cluster state, subject to the open boundary condition along the y direction with boundary at $y = k_0 + \frac{1}{2}$. As before, all the vertex d.o.f. at $y = k_0 + \frac{1}{2}$ is set to be $|+\rangle$ (see Figure 3). Additionally, we set the blue vertex d.o.f. on the interface lines in the 2D bulk to $|0\rangle$ which is one choice of the interface boundary condition in the 2D bulk. In this setting, after tracing out all bulk degrees of freedom except for the layers at $y = k_0$ and $y = k_0 + \frac{1}{2}$, the resulting state is

$$\begin{aligned} \rho_{\text{trivial|1D-DASPT}}^A \\ = \prod_{i=1}^l \left(\frac{1 + X_{i,k_0}}{2} \right) \prod_{i=1}^{l-1} \left(\frac{1 + X_{i+\frac{1}{2},k_0+\frac{1}{2}}}{2} \right) \\ \prod_{i=l+1}^{L_x-1} \left(\frac{1 + Z_{i,k_0} X_{i+\frac{1}{2},k_0+\frac{1}{2}} Z_{i+1,k_0+1}}{2} \right) \\ \left(\frac{1 + X_{l+\frac{1}{2},k_0+\frac{1}{2}} Z_{l+1,k_0}}{2} \right) \left(\frac{1 + Z_{L_x,k_0} X_{L_x+\frac{1}{2},k_0+\frac{1}{2}}}{2} \right) \\ \left(\frac{1 + Z_{l+\frac{1}{2},k_0+\frac{1}{2}} \prod_{i=l+1}^{L_x} X_{i,k_0} Z_{L_x+\frac{1}{2},k_0+\frac{1}{2}}}{2^{L_x-l}} \right). \end{aligned} \quad (42)$$

This state explicitly breaks strong $\mathbb{Z}_2^{(r)}$ symmetry to nothing but preserves the strong $\mathbb{Z}_2^{(b)}$ symmetry. This is

expected as the trivial state and the 1D-DASPT state are in different phases w.r.t. the invertible symmetries.

Alternatively, we can consider the interface state purely from the 1D perspective, i.e. by connecting together the 1D density matrices for the trivial and DASPT phases at the interface without adding additional interface terms.

$$\begin{aligned} \rho_{\text{trivial|1D-DASPT}} \\ = \prod_{i=1}^l \left(\frac{1 + X_{i,k_0}}{2} \right) \prod_{i=1}^{l-1} \left(\frac{1 + X_{i+\frac{1}{2},k_0+\frac{1}{2}}}{2} \right) \\ \prod_{i=l+1}^{L_x-1} \left(\frac{1 + Z_{i,k_0} X_{i+\frac{1}{2},k_0+\frac{1}{2}} Z_{i+1,k_0+1}}{2} \right) \\ \left(\frac{1 + Z_{l+\frac{1}{2},k_0+\frac{1}{2}} \prod_{i=l+1}^{L_x} X_{i,k_0} Z_{L_x+\frac{1}{2},k_0+\frac{1}{2}}}{2^{L_x-l}} \right). \end{aligned} \quad (43)$$

If we act with the $\mathbb{Z}_2^{(b)}$ generator $\prod_i X_{i+\frac{1}{2},k_0+\frac{1}{2}}$ on this state, we have

$$\begin{aligned} \prod_i X_{i+\frac{1}{2},k_0+\frac{1}{2}} \rho_{\text{trivial|1D-DASPT}} \\ = X_{l+\frac{1}{2},k_0+\frac{1}{2}} Z_{l+1,k_0} Z_{L_x,k_0} X_{L_x+\frac{1}{2},k_0+\frac{1}{2}} \rho_{\text{trivial|1D-DASPT}}. \end{aligned} \quad (44)$$

To make the interface state strongly symmetric under the $\mathbb{Z}_2^{(b)}$ symmetry, we need to add the projector $X_{l+\frac{1}{2},k_0+\frac{1}{2}} Z_{l+1,k_0} = \pm 1$ and $Z_{L_x,k_0} X_{L_x+\frac{1}{2},k_0+\frac{1}{2}} = \pm 1$. If we choose the sign of these projectors to be both $+1$, then we recover the state (42). The other choices correspond to tuning one or both boundary blue vertices at the two vertical lines in Figure 3 to the state $|-\rangle$. However, any such choice would explicitly break the $\mathbb{Z}_2^{(r)}$ symmetry ($\prod_i X_{i,k_0}$) to nothing. One could repeat this analysis for different choices of interface cuts (see Appendix D 1 for analysis on other choices of interface cuts). We find that it is not possible to construct an interface state that preserves all the symmetries. So any state that serves as an interface between the two states needs to explicitly break some symmetry. This is expected as the two states are in different mixed state phases w.r.t. the invertible symmetries. The interface is therefore a useful tool to diagnose different phases in this context.

B. Interface between $\rho_{\text{1D-DASPT}}^A$ and ρ_{blue}^A states: same phase w.r.t. invertible symmetries

Now let us consider an interface between the 2D cluster state and the 2D blue state, subject to open boundary condition along the y direction. As in the previous case, the d.o.f. at $y = k_0 + \frac{1}{2}$ is set to $|+\rangle$ (see Figure 3). We also set the d.o.f on the blue vertices along the two bulk interface lines to the $|+\rangle$ state. Furthermore, we decorate the two interfaces with additional $\prod_{\substack{v_b=(l+\frac{1}{2},k+\frac{1}{2}) \\ k < k_0}} CZ_{v_b,v_b+(0,1)}$ and

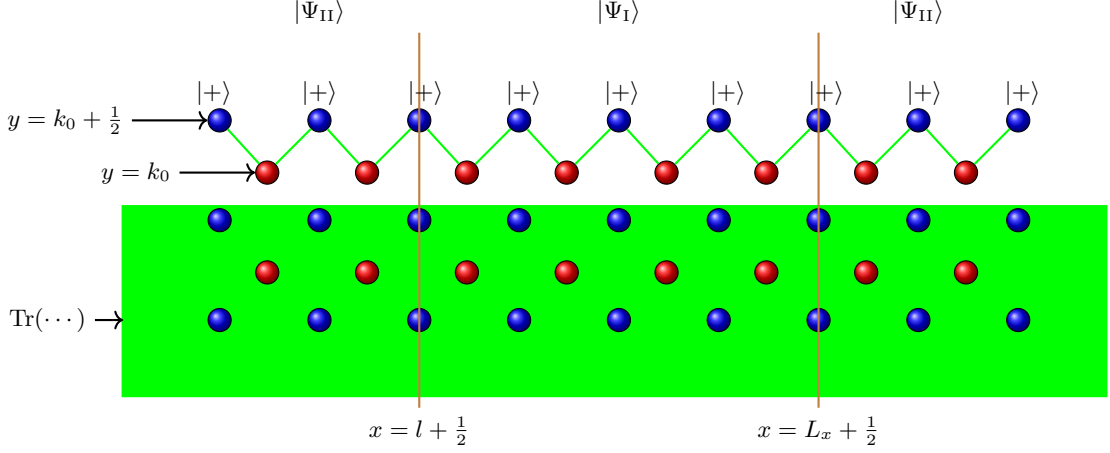


FIG. 3: Interface between two 2D states $|\Psi_I\rangle$ and $|\Psi_{II}\rangle$. We impose Dirichlet boundary condition with the boundary state to be the product state $|+\rangle^{\Delta v_b \cap A}$. After tracing out the bulk d.o.f. inside the green region, we get interfaces between the corresponding 1D states. The left vertical line is at $x = l + \frac{1}{2}$ and the right vertical line is at $L_x + \frac{1}{2}$.

$\prod_{v_b=(L_x+\frac{1}{2},k+\frac{1}{2})} CZ_{v_b,v_b+(0,1)}$. This is allowed as we are not modifying the bulk of the cluster and the blue states. This additional decoration, as we shall see, in fact gives a symmetric interface state after we trace out the 2D bulk to produce 1D mixed state. In this setting, after tracing out all bulk degrees of freedom except for the layers at $y = k_0$ and $y = k_0 + \frac{1}{2}$, the resulting state is

$$\begin{aligned} & \rho_{1D-DASPT|blue}^A \\ &= \prod_{1 \leq i \leq l-1} \left(\frac{1 + Z_{i,k_0} X_{i+\frac{1}{2},k_0+\frac{1}{2}} Z_{i+1,k_0}}{2} \right) \\ & \prod_{l+1 \leq i \leq L_x-1} \left(\frac{1 - Z_{i-\frac{1}{2},k_0+\frac{1}{2}} Y_{i,k_0} X_{i+\frac{1}{2},k_0+\frac{1}{2}} Y_{i+1,k_0} Z_{i+\frac{3}{2},k_0+\frac{1}{2}}}{2} \right) \\ & \left(\frac{1 - Z_{l,k_0} Y_{l+\frac{1}{2},k_0+\frac{1}{2}} Y_{l+1,k_0} Z_{l+\frac{3}{2},k_0+\frac{1}{2}}}{2} \right) \\ & \left(\frac{1 - Z_{L_x-\frac{1}{2},k_0+\frac{1}{2}} Y_{L_x,k_0} Y_{L_x+\frac{1}{2},k_0+\frac{1}{2}} Z_{1,k_0}}{2} \right) \left(\frac{1 + \prod_i X_{i,k_0}}{2^{|\Delta v_r \cap A|}} \right). \end{aligned} \quad (45)$$

This state has strong $\mathbb{Z}_2^{(r)} \times \mathbb{Z}_2^{(b)}$ and strong $D^{(1)}$ symmetry. Recall that, individually, both states we get after tracing out the 2D cluster state and the 2D blue state have an emergent strong $D^{(1)}$ symmetry. After we insert the above interface between these two phases, the strong $D^{(1)}$ symmetry is still maintained in this case. A summary of the features of the state $\rho_{1D-DASPT|blue}^A$ is given in Table VII.

Now suppose we consider the interface between $\rho_{1D-DASPT}^A$ and ρ_{blue}^A without adding any additional terms

on the interface, namely

$$\begin{aligned} & \rho_{1D-DASPT|blue} \\ &= \prod_{1 \leq i \leq l-1} \left(\frac{1 + Z_{i,k_0} X_{i+\frac{1}{2},k_0+\frac{1}{2}} Z_{i+1,k_0}}{2} \right) \\ & \prod_{l+1 \leq i \leq L_x-1} \left(\frac{1 - Z_{i-\frac{1}{2},k_0+\frac{1}{2}} Y_{i,k_0} X_{i+\frac{1}{2},k_0+\frac{1}{2}} Y_{i+1,k_0} Z_{i+\frac{3}{2},k_0+\frac{1}{2}}}{2} \right) \\ & \times \left(\frac{1 + \prod_i X_{i,k_0}}{2^{|\Delta v_r \cap A|}} \right). \end{aligned} \quad (46)$$

On this state, we can act with the strong symmetry

$$\prod_i X_{i,k_0} \rho_{1D-DASPT|blue} = \rho_{1D-DASPT|blue}, \quad (47a)$$

$$\begin{aligned} & \prod_i X_{i+\frac{1}{2},k_0+\frac{1}{2}} \rho_{1D-DASPT|blue} \\ &= \mathbb{X}_{l+\frac{1}{2},k_0+\frac{1}{2}} \mathbb{X}_{L_x+\frac{1}{2},k_0+\frac{1}{2}} \rho_{1D-DASPT|blue}, \end{aligned} \quad (47b)$$

where

$$\begin{aligned} & \mathbb{X}_{l+\frac{1}{2},k_0+\frac{1}{2}} \equiv Z_{l,k_0} Y_{l+\frac{1}{2},k_0+\frac{1}{2}} Y_{l+1,k_0} Z_{l+\frac{3}{2},k_0+\frac{1}{2}}, \\ & \mathbb{X}_{L_x+\frac{1}{2},k_0+\frac{1}{2}} \equiv Z_{L_x-\frac{1}{2},k_0+\frac{1}{2}} Y_{L_x,k_0} Y_{L_x+\frac{1}{2},k_0+\frac{1}{2}} Z_{1,k_0}. \end{aligned} \quad (48)$$

To make the state $\rho_{1D-DASPT|blue}$ strongly symmetric under the invertible symmetries we need to add the projectors $(1 \pm \mathbb{X}_{l+\frac{1}{2},k_0+\frac{1}{2}})/2$ and $(1 \pm \mathbb{X}_{L_x+\frac{1}{2},k_0+\frac{1}{2}})/2$. We note that the additional projectors that appear in (45), compared with (46), are exactly of the form $\mathbb{X}_{l+\frac{1}{2},k_0+\frac{1}{2}} = -1$ and $\mathbb{X}_{L_x+\frac{1}{2},k_0+\frac{1}{2}} = -1$. The other sign choices come from modifying the states of the interface blue sites in Figure 3. In any case, adding the projectors $(1 - \mathbb{X}_{l+\frac{1}{2},k_0+\frac{1}{2}})/2$ and $(1 - \mathbb{X}_{L_x+\frac{1}{2},k_0+\frac{1}{2}})/2$ make the interface state strongly symmetric under $D^{(1)}$. For other choices of interface cuts,

we can again find a symmetric interface, and leave the details to the Appendix D 2. This may indicate that $\rho_{\text{blue}}^{\text{A}}$ is in the same phase as that of $\rho_{\text{1D-DASPT}}^{\text{A}}$ if both the strong $\mathbb{Z}_2^{(r)} \times \mathbb{Z}_2^{(b)}$ symmetries and the non-invertible $\text{D}^{(1)}$ symmetry are considered. We leave further analysis for the future exploration.

C. Interface between $\rho_{\text{1D-DASPT}}^{\text{A}}$ and $\rho_{\text{blue}^{k_0;k_1}}^{\text{A}}$ states: same phase w.r.t invertible symmetries

Now let us consider an interface between the 2D cluster state and the 2D blue $^{k_0;k_1}$ state, subject to open boundary condition along the y direction. As in the previous case, the d.o.f. at $y = k_0 + \frac{1}{2}$ are set to $|+\rangle$. Like in the previous section, we also set the d.o.f on the blue vertices along the two bulk interface lines to the $|+\rangle$ state. Furthermore, we decorate the two interfaces with additional $\prod_{v_b=(l+\frac{1}{2},k+\frac{1}{2})}^{k < k_0} CZ_{v_b, v_b+(0,1)}$ and $\prod_{v_b=(L_x+\frac{1}{2},k+\frac{1}{2})}^{k < k_0} CZ_{v_b, v_b+(0,1)}$. In this setting, after tracing out all bulk degrees of freedom except for the layers at $y = k_0$ and $y = k_0 + \frac{1}{2}$, the resulting state is

$$\begin{aligned} & \rho_{\text{1D-DASPT}|\text{blue}^{k_0;k_1}}^{\text{A}} \\ = & \prod_{1 \leq i \leq l-1} \left(\frac{1 + Z_{i,k_0} X_{i+\frac{1}{2},k_0+\frac{1}{2}} Z_{i+1,k_0}}{2} \right) \\ & \prod_{l+1 \leq i \leq L_x-1} \left(\frac{1 - Y_{i,k_0} X_{i+\frac{1}{2},k_0+\frac{1}{2}} Y_{i+1,k_0}}{2} \right) \\ & \left(\frac{1 - Z_{l,k_0} Y_{l+\frac{1}{2},k_0+\frac{1}{2}} Y_{l+1,k_0}}{2} \right) \left(\frac{1 - Y_{L_x,k_0} Y_{L_x+\frac{1}{2},k_0+\frac{1}{2}} Z_{1,k_0}}{2} \right) \\ & \times \left(\frac{1 + \prod_i X_{i,k_0}}{2^{|\Delta_{v_r, \cap A}|}} \right). \end{aligned} \quad (49)$$

This state has strong $\mathbb{Z}_2^{(r)} \times \mathbb{Z}_2^{(b)}$ symmetry. A summary of the features of the state $\rho_{\text{1D-DASPT}|\text{blue}^{k_0;k_1}}^{\text{A}}$ is given in Table VIII.

Now suppose we consider the interface between $\rho_{\text{1D-DASPT}}^{\text{A}}$ and $\rho_{\text{blue}^{k_0;k_1}}^{\text{A}}$ without adding any additional terms on the interface

$$\begin{aligned} & \rho_{\text{1D-DASPT}|\text{blue}^{k_0;k_1}} \\ = & \prod_{1 \leq i \leq l-1} \left(\frac{1 + Z_{i,k_0} X_{i+\frac{1}{2},k_0+\frac{1}{2}} Z_{i+1,k_0}}{2} \right) \\ & \prod_{l+1 \leq i \leq L_x-1} \left(\frac{1 - Y_{i,k_0} X_{i+\frac{1}{2},k_0+\frac{1}{2}} Y_{i+1,k_0}}{2} \right) \\ & \times \left(\frac{1 + \prod_i X_{i,k_0}}{2^{|\Delta_{v_r, \cap A}|}} \right). \end{aligned} \quad (50)$$

On this state, we can act with the strong symmetry

$$\begin{aligned} & \prod_i X_{i,k_0} \rho_{\text{1D-DASPT}|\text{blue}^{k_0;k_1}} \\ = & \rho_{\text{1D-DASPT}|\text{blue}^{k_0;k_1}}, \end{aligned} \quad (51a)$$

$$\begin{aligned} & \prod_i X_{i+\frac{1}{2},k_0+\frac{1}{2}} \rho_{\text{1D-DASPT}|\text{blue}^{k_0;k_1}} \\ = & \mathbb{X}_{l+\frac{1}{2},k_0+\frac{1}{2}} \mathbb{X}_{L_x+\frac{1}{2},k_0+\frac{1}{2}} \rho_{\text{1D-DASPT}|\text{blue}^{k_0;k_1}}, \end{aligned} \quad (51b)$$

where

$$\begin{aligned} \mathbb{X}_{l+\frac{1}{2},k_0+\frac{1}{2}} & \equiv Z_{l,k_0} X_{l+\frac{1}{2},k_0+\frac{1}{2}} Y_{l+1,k_0}, \\ \mathbb{X}_{L_x+\frac{1}{2},k_0+\frac{1}{2}} & \equiv Y_{L_x,k_0} X_{L_x+\frac{1}{2},k_0+\frac{1}{2}} Z_{1,k_0}. \end{aligned} \quad (52)$$

To make the state $\rho_{\text{1D-DASPT}|\text{blue}^{k_0;k_1}}$ strongly symmetric under the $\mathbb{Z}_2^{(r)} \times \mathbb{Z}_2^{(b)}$ symmetry, we can add the projectors $(1 \pm \mathbb{X}_{l+\frac{1}{2},k_0+\frac{1}{2}})/2$ and $(1 \pm \mathbb{X}_{L_x+\frac{1}{2},k_0+\frac{1}{2}})/2$. This indicates that $\rho_{\text{1D-DASPT}}^{\text{A}}$ and $\rho_{\text{blue}^{k_0;k_1}}^{\text{A}}$ are in the same phase as far as the $\mathbb{Z}_2^{(r)} \times \mathbb{Z}_2^{(b)}$ strong symmetries are considered. However, these two phases are distinguished by the non-invertible $\text{D}^{(1)}$ symmetry, since $\rho_{\text{1D-DASPT}}^{\text{A}}$ has strong $\text{D}^{(1)}$ symmetry while $\rho_{\text{blue}^{k_0;k_1}}^{\text{A}}$ is not symmetric under $\text{D}^{(1)}$. We leave the analysis of other interface cuts to the Appendix D 3.

VI. Conclusion

In this work, we have investigated a variety of 1D mixed-state phases obtained by tracing out the 2D bulk degrees of freedom. When the bulk is a 2D higher-order SSPT, we obtain 1D DASPTs, which display a coexistence of mSPT order and SWSSB. A numerical study of DASPTs was carried out in [65]. In the specific examples we consider, these phases are characterized by a nonzero Rényi-2 (or fidelity) correlator signaling SWSSB, and a nonzero expectation value of string order parameters, indicating mixed-state SPT order. We note that the existence of both SPT and SSB order in pure states has been explored in [67, 68], and in non-equilibrium settings in [69].

To characterize and distinguish these 1D mSPT phases, we employed interfaces as diagnostic probes. We showed by explicit examples that when two mixed states belong to the same phase, there exists an interface interpolation between them that preserves all the symmetries under consideration. When there is no local modification to preserve the symmetries across the interface, the two sides are in distinct phases.

An important future direction is to establish, on general grounds, that interfaces provide a universal and robust probe for distinguishing mSPT phases. In this manuscript, we presented several concrete examples demonstrating how interfaces can be used to differentiate between distinct mSPT phases. It would be particularly valuable to connect this interface-based diagnostic to the

formal definition of mSPT phases in terms of two-way symmetric finite-depth local quantum channels.

Furthermore, we found that there exists an interface interpolation between $\rho_{\text{1D-DASPT}}$ and ρ_{blue} that is symmetric under the strong $\mathbb{Z}_2^{(r)} \times \mathbb{Z}_2^{(b)}$ symmetry as well as the strong non-invertible $D^{(1)}$ symmetry. This observation motivates an interesting open problem: if they are indeed in the same phase, how could we explicitly construct a symmetric finite-depth local quantum channel that connects $\rho_{\text{1D-DASPT}}$ and ρ_{blue} ? Such a construction would provide a concrete realization of the equivalence between these phases and further clarify the role of interface as a probe to distinguish between mSPT phases.

Note: While preparing this manuscript, a work ap-

peared on the arXiv presenting a systematic understanding of 1D mixed-state phases with $\mathbb{Z}_2 \times \mathbb{Z}_2$ symmetry from an alternative purification perspective [73].

Acknowledgment

The authors thank Arkya Chatterjee, Yabo Li, Ruochen Ma, Shijun Sun, and Jian-Hao Zhang for helpful discussions. FY thanks the Simons Center for Geometry and Physics at Stony Brook University for great hospitality during various stages of this work. This work was supported by the U.S. Department of Energy, Office of Basic Energy Sciences, under Contract No. DE-SC0012704 (APM, FY & TCW) and the National Science Foundation under Grant No. DRL I-TEST 2148467 (ZS).

-
- [1] X. Chen, Z.-X. Liu, and X.-G. Wen, Two-dimensional symmetry-protected topological orders and their protected gapless edge excitations, *Phys. Rev. B* **84**, 235141 (2011), [arXiv:1106.4752 \[cond-mat.str-el\]](#).
- [2] X. Chen, Z.-C. Gu, Z.-X. Liu, and X.-G. Wen, Symmetry protected topological orders and the group cohomology of their symmetry group, *Phys. Rev. B* **87**, 155114 (2013), [arXiv:1106.4772 \[cond-mat.str-el\]](#).
- [3] X. Chen, Z.-C. Gu, Z.-X. Liu, and X.-G. Wen, Symmetry-protected topological orders in interacting bosonic systems, *Science* **338**, 1604 (2012).
- [4] Z.-C. Gu and X.-G. Wen, Symmetry-protected topological orders for interacting fermions: Fermionic topological nonlinear σ models and a special group supercohomology theory, *Physical Review B* **90**, 115141 (2014).
- [5] A. Kapustin, Symmetry Protected Topological Phases, Anomalies, and Cobordisms: Beyond Group Cohomology (2014), [arXiv:1403.1467 \[cond-mat.str-el\]](#).
- [6] As these two terms appear in the literature, so we will use mSPT and ASPT interchangeably.
- [7] C. de Groot, A. Turzillo, and N. Schuch, Symmetry Protected Topological Order in Open Quantum Systems, *Quantum* **6**, 856 (2022).
- [8] R. Ma and C. Wang, Average symmetry-protected topological phases, *Phys. Rev. X* **13**, 031016 (2023).
- [9] R. Ma, J.-H. Zhang, Z. Bi, M. Cheng, and C. Wang, Topological phases with average symmetries: The decohered, the disordered, and the intrinsic, *Phys. Rev. X* **15**, 021062 (2025).
- [10] R. Fan, Y. Bao, E. Altman, and A. Vishwanath, Diagnostics of mixed-state topological order and breakdown of quantum memory, *PRX Quantum* **5**, 020343 (2024).
- [11] J. Y. Lee, Y.-Z. You, and C. Xu, Symmetry protected topological phases under decoherence, *Quantum* **9**, 1607 (2025).
- [12] J.-H. Zhang, Y. Qi, and Z. Bi, Fidelity Strange Correlators for Average Symmetry-Protected Topological Phases (2022), [arXiv:2210.17485 \[cond-mat.str-el\]](#).
- [13] J. Y. Lee, C.-M. Jian, and C. Xu, Quantum criticality under decoherence or weak measurement, *PRX Quantum* **4**, 030317 (2023).
- [14] R. Ma and A. Turzillo, Symmetry-protected topological phases of mixed states in the doubled space, *PRX Quantum* **6**, 010348 (2025).
- [15] H. Xue, J. Y. Lee, and Y. Bao, Tensor network formulation of symmetry protected topological phases in mixed states (2024), [arXiv:2403.17069 \[cond-mat.str-el\]](#).
- [16] Y. Guo, J.-H. Zhang, H.-R. Zhang, S. Yang, and Z. Bi, Locally purified density operators for symmetry-protected topological phases in mixed states, *Phys. Rev. X* **15**, 021060 (2025).
- [17] J. Guo, O. Hart, C.-F. Chen, A. J. Friedman, and A. Lucas, Designing open quantum systems with known steady states: Davies generators and beyond, *Quantum* **9**, 1612 (2025).
- [18] Y.-H. Chen and T. Grover, Symmetry-enforced many-body separability transitions, *PRX Quantum* **5**, 030310 (2024).
- [19] L. A. Lessa, M. Cheng, and C. Wang, Mixed-state quantum anomaly and multipartite entanglement, *Phys. Rev. X* **15**, 011069 (2025).
- [20] Z. Wang, Z. Wu, and Z. Wang, Intrinsic mixed-state topological order, *PRX Quantum* **6**, 010314 (2025).
- [21] Z. Wang and L. Li, Anomaly in open quantum systems and its implications on mixed-state quantum phases, *PRX Quantum* **6**, 010347 (2025).
- [22] P. Sala, S. Gopalakrishnan, M. Oshikawa, and Y. You, Spontaneous strong symmetry breaking in open systems: Purification perspective, *Phys. Rev. B* **110**, 155150 (2024).
- [23] L. A. Lessa, R. Ma, J.-H. Zhang, Z. Bi, M. Cheng, and C. Wang, Strong-to-Weak Spontaneous Symmetry Breaking in Mixed Quantum States, *PRX Quantum* **6**, 010344 (2025), [arXiv:2405.03639 \[quant-ph\]](#).
- [24] X. Huang, M. Qi, J.-H. Zhang, and A. Lucas, Hydrodynamics as the effective field theory of strong-to-weak spontaneous symmetry breaking, *Phys. Rev. B* **111**, 125147 (2025).
- [25] Z. Zhang, U. Agrawal, and S. Vijay, Quantum communication and mixed-state order in decohered symmetry-protected topological states, *Phys. Rev. B* **111**, 115141 (2025).

- [26] J.-H. Zhang, C. Xu, and Y. Xu, Fluctuation-Dissipation Theorem and Information Geometry in Open Quantum Systems (2024), [arXiv:2409.18944 \[quant-ph\]](#).
- [27] T. D. Ellison and M. Cheng, Toward a classification of mixed-state topological orders in two dimensions, *PRX Quantum* **6**, 010315 (2025).
- [28] R. Sohal and A. Prem, Noisy approach to intrinsically mixed-state topological order, *PRX Quantum* **6**, 010313 (2025).
- [29] C. Zhang, Y. Xu, J.-H. Zhang, C. Xu, Z. Bi, and Z.-X. Luo, Strong-to-weak spontaneous breaking of 1-form symmetry and intrinsically mixed topological order, *Phys. Rev. B* **111**, 115137 (2025).
- [30] P. Sala, J. Alicea, and R. Verresen, Decoherence and wave-function deformation of D_4 non-abelian topological order, *Phys. Rev. X* **15**, 031002 (2025).
- [31] Z. Song and J.-H. Zhang, Strong-to-weak spontaneous symmetry breaking of higher-form non-invertible symmetries in Kitaev's quantum double model (2025), [arXiv:2509.24179 \[quant-ph\]](#).
- [32] S. Sun, J.-H. Zhang, Z. Bi, and Y. You, Holographic View of Mixed-State Symmetry-Protected Topological Phases in Open Quantum Systems, *PRX Quantum* **6**, 020333 (2025), [arXiv:2410.08205 \[quant-ph\]](#).
- [33] X.-Q. Sun, Anomalous matrix product operator symmetries and 1D mixed-state phases (2025), [arXiv:2504.16985 \[quant-ph\]](#).
- [34] S. Sang, Y. Zou, and T. H. Hsieh, Mixed-state quantum phases: Renormalization and quantum error correction, *Phys. Rev. X* **14**, 031044 (2024).
- [35] S. Sang and T. H. Hsieh, Stability of Mixed-State Quantum Phases via Finite Markov Length, *Phys. Rev. Lett.* **134**, 070403 (2025), [arXiv:2404.07251 \[quant-ph\]](#).
- [36] D. Gu, Z. Wang, and Z. Wang, Spontaneous symmetry breaking in open quantum systems: Strong, weak, and strong-to-weak, *Phys. Rev. B* **112**, 245123 (2025).
- [37] Y. Guo, K. Ding, and S. Yang, A new framework for quantum phases in open systems: steady state of imaginary-time lindbladian evolution, *Reports on Progress in Physics* **88**, 118001 (2025).
- [38] R. Luo, Y.-N. Wang, and Z. Bi, Topological holography for mixed-state phases and phase transitions, *PRX Quantum* **6**, 040358 (2025).
- [39] S. Schafer-Nameki, A. Tiwari, A. Warman, and C. Zhang, SymTFT Approach for Mixed States with Non-Invertible Symmetries (2025), [arXiv:2507.05350 \[quant-ph\]](#).
- [40] M. Qi, R. Sohal, X. Chen, D. T. Stephen, and A. Prem, The Symmetry Taco: Equivalences between Gapped, Gapless, and Mixed-State SPTs (2025), [arXiv:2507.05335 \[cond-mat.str-el\]](#).
- [41] B. Aldossari, S. Blinov, and Z.-X. Luo, Tensor Network Representations for Intrinsically Mixed-State Topological Orders (2025), [arXiv:2507.22989 \[cond-mat.str-el\]](#).
- [42] T.-H. Yang, B. Shi, and J. Y. Lee, Topological Mixed States: Phases of Matter from Axiomatic Approaches (2025), [arXiv:2506.04221 \[cond-mat.str-el\]](#).
- [43] R. Ma, V. Khemani, and S. Sang, Circuit-based characterization of finite-temperature quantum phases and self-correcting quantum memory (2025), [arXiv:2509.15204 \[quant-ph\]](#).
- [44] S. Sang, L. A. Lessa, R. S. K. Mong, T. Grover, C. Wang, and T. H. Hsieh, Mixed-state phases from local reversibility (2025), [arXiv:2507.02292 \[quant-ph\]](#).
- [45] T.-C. Lu, Y.-J. Liu, S. Gopalakrishnan, and Y. You, Holographic duality between bulk topological order and boundary mixed-state order (2025), [arXiv:2511.19597 \[quant-ph\]](#).
- [46] J. Hauser, K. Su, H. Ha, J. Lloyd, T. G. Kiely, R. Vasseur, S. Gopalakrishnan, C. Xu, and M. P. A. Fisher, Strong-to-weak symmetry breaking in open quantum systems: From discrete particles to continuum hydrodynamics (2026), [arXiv:2602.16045 \[quant-ph\]](#).
- [47] S. Roberts, B. Yoshida, A. Kubica, and S. D. Bartlett, Symmetry-protected topological order at nonzero temperature, *Phys. Rev. A* **96**, 022306 (2017).
- [48] O. Viyuela, A. Rivas, and M. A. Martin-Delgado, Symmetry-protected topological phases at finite temperature, *2D Materials* **2**, 034006 (2015).
- [49] C. Fechin, N. Tantivasadakarn, and V. V. Albert, Non-invertible Symmetry-Protected Topological Order in a Group-Based Cluster State, *Phys. Rev. X* **15**, 011058 (2025), [arXiv:2312.09272 \[cond-mat.str-el\]](#).
- [50] S. Seifnashri and S.-H. Shao, Cluster State as a Non-invertible Symmetry-Protected Topological Phase, *Phys. Rev. Lett.* **133**, 116601 (2024), [arXiv:2404.01369 \[cond-mat.str-el\]](#).
- [51] Y. Li and M. Litvinov, Non-invertible SPT, gauging and symmetry fractionalization (2024), [arXiv:2405.15951 \[cond-mat.str-el\]](#).
- [52] K. Inamura and S. Ohyama, 1+1d SPT phases with fusion category symmetry: interface modes and non-abelian Thouless pump (2024), [arXiv:2408.15960 \[cond-mat.str-el\]](#).
- [53] C. Meng, X. Yang, T. Lan, and Z. Gu, Non-invertible SPTs: an on-site realization of (1+1)d anomaly-free fusion category symmetry (2024), [arXiv:2412.20546 \[cond-mat.str-el\]](#).
- [54] Y. Choi, Y. Sanghavi, S.-H. Shao, and Y. Zheng, Non-invertible and higher-form symmetries in 2+1d lattice gauge theories, *SciPost Phys.* **18**, 008 (2025), [arXiv:2405.13105 \[cond-mat.str-el\]](#).
- [55] Z. Jia, Generalized cluster states from Hopf algebras: non-invertible symmetry and Hopf tensor network representation, *JHEP* **09**, 147, [arXiv:2405.09277 \[quant-ph\]](#).
- [56] S. D. Pace, H. T. Lam, and O. M. Aksoy, (SPT-)LSM theorems from projective non-invertible symmetries, *SciPost Phys.* **18**, 028 (2025), [arXiv:2409.18113 \[cond-mat.str-el\]](#).
- [57] L. Li, R.-Z. Huang, and W. Cao, Noninvertible symmetry-enriched quantum critical point, *Phys. Rev. B* **112**, L081113 (2025), [arXiv:2411.19034 \[cond-mat.str-el\]](#).
- [58] Z. Jia, Weak Hopf non-invertible symmetry-protected topological spin liquid and lattice realization of (1+1)D symmetry topological field theory (2024), [arXiv:2412.15336 \[hep-th\]](#).
- [59] Z. Jia, Quantum Cluster State Model with Haagerup Fusion Category Symmetry (2024), [arXiv:2412.19657 \[math.QA\]](#).
- [60] W. Cao, M. Yamazaki, and L. Li, Duality viewpoint of noninvertible symmetry protected topological phases (2025), [arXiv:2502.20435 \[cond-mat.str-el\]](#).
- [61] D.-C. Lu, F. Xu, and Y.-Z. You, Strange correlator and string order parameter for non-invertible symmetry protected topological phases in 1+1d (2025), [arXiv:2505.00673 \[cond-mat.str-el\]](#).
- [62] O. M. Aksoy and X.-G. Wen, Phases with non-invertible symmetries in 1+1D symmetry protected topological orders as duality automorphisms (2025), [arXiv:2503.21764](#)

- [cond-mat.str-el].
- [63] A. Parayil Mana, Y. Li, H. Sukeno, and T.-C. Wei, Higher-order topological phases protected by non-invertible and subsystem symmetries (2025), [arXiv:2505.18119](#) [cond-mat.str-el].
- [64] Y. Kuno, T. Orito, and I. Ichinose, Strong-to-weak spontaneous symmetry breaking and average symmetry protected topological order in the doubled Hilbert space, *Phys. Rev. B* **111**, 174110 (2025), [arXiv:2503.10311](#) [quant-ph].
- [65] Y. Guo and S. Yang, Strong-to-weak spontaneous symmetry breaking meets average symmetry-protected topological order, *Phys. Rev. B* **111**, L201108 (2025).
- [66] A. Parayil Mana, Y. Li, H. Sukeno, and T.-C. Wei, Kennedy-Tasaki transformation and noninvertible symmetry in lattice models beyond one dimension, *Phys. Rev. B* **109**, 245129 (2024), [arXiv:2402.09520](#) [cond-mat.str-el].
- [67] R. Verresen, R. Moessner, and F. Pollmann, One-dimensional symmetry protected topological phases and their transitions, *Phys. Rev. B* **96**, 165124 (2017), [arXiv:1707.05787](#) [cond-mat.str-el].
- [68] B. Zeng and D.-L. Zhou, Topological and error-correcting properties for symmetry-protected topological order, *EPL* **113**, 56001 (2016), [arXiv:1407.3413](#) [quant-ph].
- [69] R. Morral-Yepes, F. Pollmann, and I. Lovas, Detecting and stabilizing measurement-induced symmetry-protected topological phases in generalized cluster models, *Phys. Rev. B* **108**, 224304 (2023), [arXiv:2302.14551](#) [quant-ph].
- [70] N. Seiberg and S.-H. Shao, Majorana chain and Ising model – (non-invertible) translations, anomalies, and emanant symmetries, *SciPost Phys.* **16**, 064 (2024), [arXiv:2307.02534](#) [cond-mat.str-el].
- [71] X. Chen, A. Dua, M. Hermele, D. T. Stephen, N. Tantivasadakarn, R. Vanhove, and J.-Y. Zhao, Sequential quantum circuits as maps between gapped phases, *Phys. Rev. B* **109**, 075116 (2024), [arXiv:2307.01267](#) [cond-mat.str-el].
- [72] W. W. Ho and T. H. Hsieh, Efficient variational simulation of non-trivial quantum states, *SciPost Phys.* **6**, 029 (2019), [arXiv:1803.00026](#).
- [73] Y. Guo and S. Yang, Quantum criticality in open quantum systems from the purification perspective (2026), [arXiv:2602.21979](#) [quant-ph].
- [74] C. Meng, X. Yang, T. Lan, and Z. Gu, Non-invertible SPTs: an on-site realization of (1+1)d anomaly-free fusion category symmetry (2024), [arXiv:2412.20546](#) [cond-mat.str-el].
- [75] C.-M. Chang, Y.-H. Lin, S.-H. Shao, Y. Wang, and X. Yin, Topological Defect Lines and Renormalization Group Flows in Two Dimensions, *JHEP* **01**, 026, [arXiv:1802.04445](#) [hep-th].

A. Extra examples

1. Mixed state from 2D cluster state

In this section, we look at the states obtained by tracing out the 2D cluster state on a torus and on a cylinder with generic boundary condition. The results are summarized in Table I.

a. 2D cluster state on a torus

We assume periodic boundary conditions for both x and y directions for the cluster Hamiltonian. Now we trace out all the 2D d.o.f. except the rows with $y = k$ and $y = k + \frac{1}{2}$. Let us call this region A and the rest of the rows as A^c (see Figure 4). Tracing over the region A^c give

$$\begin{aligned}
& \text{Tr}_{A^c} (|2\text{D-cluster}\rangle \langle 2\text{D-cluster}|) \\
&= \frac{4}{2^{|\Delta_{v_r} \cup \Delta_{v_b} \cap A|}} \sum_{\substack{\{i_l\} \subset \Delta_{v_r} \cap A, \\ \{j_l\} \subset \Delta_{v_b} \cap A \\ r, s \text{ even}}} Z_{i_1} \dots Z_{i_r} Z_{j_1} \dots Z_{j_s} |1\text{D-cluster}\rangle \langle 1\text{D-cluster}| Z_{i_1} \dots Z_{i_r} Z_{j_1} \dots Z_{j_s} \\
&= \frac{(1 + \prod_i X_{i,k}) (1 + \prod_i X_{i+\frac{1}{2}, k+\frac{1}{2}})}{2^{|\Delta_{v_r} \cap A|} 2^{|\Delta_{v_b} \cap A|}} \\
&\equiv \rho_{1\text{D-SWSSB}}^A,
\end{aligned} \tag{A1}$$

where $\{i_l\}$ and $\{j_l\}$ are subset of vertices in $\Delta_{v_r} \cap A$ and $\Delta_{v_b} \cap A$ respectively and the 1D cluster state is along the region A

$$|1\text{D-cluster}\rangle = \prod_i CZ_{(i+\frac{1}{2}, k+\frac{1}{2}), (i, k)} |+\rangle^{\otimes \Delta_{v_r} \cap A} |+\rangle^{\otimes \Delta_{v_b} \cap A}. \tag{A2}$$

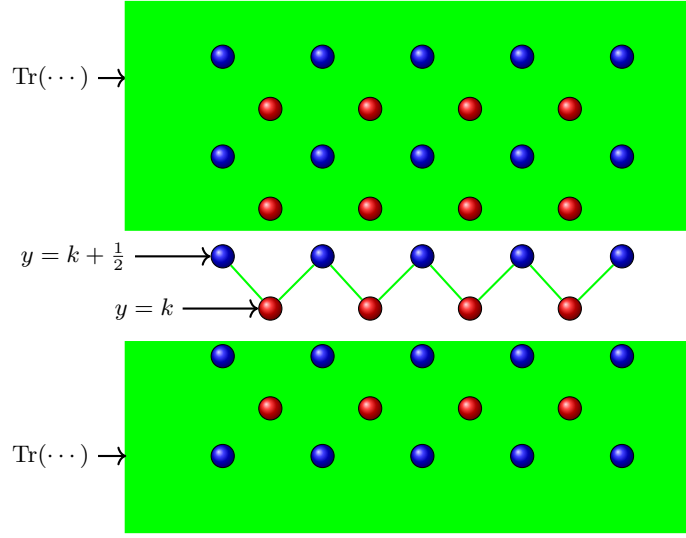


FIG. 4: The vertices in the region A are at $y = k$ and $y = k + \frac{1}{2}$. The green line connecting red and blue vertices in region A indicate the CZ gates that remain after tracing out A^c . The green region contains the d.o.f. that we trace over.

We note that $\rho_{\text{1D-SWSSB}}^A$ has strong $\mathbb{Z}_2^{(r)} \times \mathbb{Z}_2^{(b)}$ 0-form symmetry generated by $\eta_{r,k}^x$ and $\eta_{b,k}^x$, i.e,

$$\eta_{r,k}^x \rho_{\text{1D-SWSSB}}^A = \rho_{\text{1D-SWSSB}}^A, \quad (\text{A3a})$$

$$\eta_{b,k}^x \rho_{\text{1D-SWSSB}}^A = \rho_{\text{1D-SWSSB}}^A. \quad (\text{A3b})$$

This state has the following weak stabilizers

$$Z_{i,k} X_{i+\frac{1}{2},k+\frac{1}{2}} Z_{i+1,k} \rho_{\text{1D-SWSSB}}^A Z_{i,k} X_{i+\frac{1}{2},k+\frac{1}{2}} Z_{i+1,k} = \rho_{\text{1D-SWSSB}}^A, \quad (\text{A4a})$$

$$Z_{i-\frac{1}{2},k+\frac{1}{2}} X_{i,k} Z_{i+\frac{1}{2},k+\frac{1}{2}} \rho_{\text{1D-SWSSB}}^A Z_{i-\frac{1}{2},k+\frac{1}{2}} X_{i,k} Z_{i+\frac{1}{2},k+\frac{1}{2}} = \rho_{\text{1D-SWSSB}}^A. \quad (\text{A4b})$$

Interestingly, $\rho_{\text{1D-SWSSB}}^A$ has weak non-invertible symmetry $D^{(1)}$ defined in (24). Weak non-invertible symmetry satisfies

$$D^{(1)} \rho_{\text{1D-SWSSB}}^A (D^{(1)})^\dagger = \rho_{\text{1D-SWSSB}}^A. \quad (\text{A5})$$

We note that $Z_{i,k}$ and $Z_{i+\frac{1}{2},k+\frac{1}{2}}$ are good order parameters for the symmetries $\eta_{r,k}^x$ and $\eta_{b,k}^x$ respectively as they anti-commute with the symmetry operators. Using the fidelity correlator and Rényi-2 correlator defined in [23], it can be easily verified that $\rho_{\text{1D-SWSSB}}^A$ is SWSSB of the $\mathbb{Z}_2^{(r)} \times \mathbb{Z}_2^{(b)}$ symmetry. Concretely, for the Rényi-2 correlators we have:

$$\begin{aligned} \text{Tr} \left(Z_{i,k} Z_{j,k} \rho_{\text{1D-SWSSB}}^A Z_{i,k} Z_{j,k} \rho_{\text{1D-SWSSB}}^A \right) &= 1, \\ \text{Tr} \left(Z_{i+\frac{1}{2},k+\frac{1}{2}} Z_{j+\frac{1}{2},k+\frac{1}{2}} \rho_{\text{1D-SWSSB}}^A Z_{i+\frac{1}{2},k+\frac{1}{2}} Z_{j+\frac{1}{2},k+\frac{1}{2}} \rho_{\text{1D-SWSSB}}^A \right) &= 1. \end{aligned} \quad (\text{A6})$$

while for fidelity correlators we have:

$$\begin{aligned} \text{Tr} \left(\sqrt{\rho_{\text{1D-SWSSB}}^A} Z_{i,k} Z_{j,k} \rho_{\text{1D-SWSSB}}^A Z_{i,k} Z_{j,k} \sqrt{\rho_{\text{1D-SWSSB}}^A} \right) &= 1, \\ \text{Tr} \left(\sqrt{\rho_{\text{1D-SWSSB}}^A} Z_{i+\frac{1}{2},k+\frac{1}{2}} Z_{j+\frac{1}{2},k+\frac{1}{2}} \rho_{\text{1D-SWSSB}}^A Z_{i+\frac{1}{2},k+\frac{1}{2}} Z_{j+\frac{1}{2},k+\frac{1}{2}} \sqrt{\rho_{\text{1D-SWSSB}}^A} \right) &= 1. \end{aligned} \quad (\text{A7})$$

b. 2D cluster state on a semi-infinite cylinder with generic boundary condition

We consider the Hamiltonian $H_{\text{2D-cluster}}$ on a cylinder, i.e, open boundary condition on the y direction with top boundary ending at the row of blue vertices. The y coordinate takes values from $-\infty$ to $1, \dots, k_0, k_0 + \frac{1}{2}$. Now we trace

out all the 2D d.o.f. except for the top rows at $y = k_0$ and $y = k_0 + \frac{1}{2}$ (we call the top rows again region A). Tracing out A^c gives

$$\begin{aligned} & \text{Tr}_{A^c} (|2\text{D-cluster}\rangle \langle 2\text{D-cluster}|) \\ &= \frac{2}{2^{|\Delta_{v_r} \cap A|}} \sum_{\substack{\{i\} \in \Delta_{v_r} \cap A, \\ r \text{ even}}} Z_{i_1} \dots Z_{i_r} \prod CZ_{v_r, v_b} |+\rangle^{\otimes \Delta_{v_r}} |\phi\rangle^{\otimes \Delta_{v_b}} \langle \phi|^{\otimes \Delta_{v_b}} \langle +|^{\otimes \Delta_{v_r}} \prod CZ_{v_r, v_b} Z_{i_1} \dots Z_{i_r} \\ &\equiv \rho_{1\text{D-SWSSB}_r}^A, \end{aligned} \quad (\text{A8})$$

where the $|\phi\rangle^{\otimes \Delta_{v_b}}$ are dangling d.o.f.s. The above state has strong $\mathbb{Z}_2^{(r)}$ symmetry = $\prod_i X_{i, k_0}$ 0-form symmetry. In addition, we have the weak stabilizers

$$Z_{i-\frac{1}{2}, k_0+\frac{1}{2}} X_{i, k_0} Z_{i+\frac{1}{2}, k_0+\frac{1}{2}} \rho_{1\text{D-SWSSB}}^A Z_{i-\frac{1}{2}, k_0+\frac{1}{2}} X_{i, k_0} Z_{i+\frac{1}{2}, k_0+\frac{1}{2}} = \rho_{1\text{D-SWSSB}}^A. \quad (\text{A9})$$

$\rho_{1\text{D-SWSSB}}^A$ is in the SWSSB phase regarding the $\mathbb{Z}_2^{(r)}$ symmetry. This can be checked using the fidelity correlator or the Rényi-2 correlator, both of which evaluate to 1 if we take Z_{i, k_0} as the order parameter.

c. Tracing the interface between 2D trivial state and 2D cluster state on a torus

Let us consider the two dimensional state that constitute an interface between the 2D trivial state and 2D cluster state, subject to periodic boundary condition along the y direction. We take the interface to lie along the lines $x = l + \frac{1}{2}$ and $x = L_x + \frac{1}{2}$. After tracing out the bulk degrees of freedom except for the layers at $y = k$ and $y = k + \frac{1}{2}$, the resulting reduced density matrix is identical to trivial state in one region and identical to the $\rho_{1\text{D-SWSSB}}^A$ in the other region. Equivalently, this can be thought of as $\rho_{1\text{D-SWSSB}}^A$ with open boundary condition. Otherwise, the strong $\mathbb{Z}_2^{(r)}$ symmetry is explicitly broken to weak symmetry and strong $\mathbb{Z}_2^{(b)}$ symmetry is broken to nothing unless we fine tune the state at $(x, y) = (l + \frac{1}{2}, k + \frac{1}{2})$ and $(x, y) = (L_x + \frac{1}{2}, k + \frac{1}{2})$.

d. Tracing the interface between 2D trivial state and 2D cluster state on a cylinder with generic open boundary condition

Let us consider the two dimensional state that constitute an interface between the 2D trivial state and 2D cluster state, subject to open boundary condition along the y direction. We take the boundary to lie at $y = k_0$ and $y = k_0 + \frac{1}{2}$. We take the interface to lie along the lines $x = l + \frac{1}{2}$ and $x = L_x + \frac{1}{2}$. After tracing out the bulk degrees of freedom except for the layers at $y = k_0$ and $y = k_0 + \frac{1}{2}$, the resulting reduced density matrix is identical to trivial state in one region and identical to the $\rho_{1\text{D-SWSSB}_r}^A$ in the other region. Equivalently, this can be thought of as $\rho_{1\text{D-SWSSB}_r}^A$ with open boundary condition. Otherwise, the strong $\mathbb{Z}_2^{(r)}$ symmetry is explicitly broken to weak symmetry.

2. Mixed state from 2D blue state

In this section, we look at the states obtained by tracing out the 2D blue state on a torus and on a cylinder with generic boundary condition. The results are summarized in Table III.

a. 2D blue state on a torus

In this section, we place the blue state on a torus and trace out all the bulk d.o.f. except at $y = k$ and $y = k + \frac{1}{2}$. As before, we denote these rows as A and the rest as A^c . Tracing out A^c gives

$$\begin{aligned} \text{Tr}_{A^c} (|\text{blue}\rangle \langle \text{blue}|) &= \frac{4}{2^{|\Delta_{v_b} \cap A| + |\Delta_{v_r} \cap A|}} \sum_{\substack{\{i\} \in \Delta_{v_r} \cap A, \\ r, s \text{ even}}} Z_{i_1} \dots Z_{i_r} Z_{j_1} \dots Z_{j_s} |1\text{D-cluster}\rangle \langle 1\text{D-cluster}| Z_{i_1} \dots Z_{i_r} Z_{j_1} \dots Z_{j_s} \\ &= \rho_{1\text{D-SWSSB}}^A, \end{aligned} \quad (\text{A10})$$

where the |1D-cluster) is given in (A2). Here, it seems that by tracing out the region A^c , we lose information about the distinction between |blue) ⟨blue| and |2D-cluster) ⟨2D-cluster|. Moreover, $\rho_{1D-SWSSB}^A$, which appeared previously in (A1), is in the SWSSB phase regarding the $\mathbb{Z}_2^{(r)} \times \mathbb{Z}_2^{(b)}$ symmetries. We verified this by computing the Rényi-2 correlator and the fidelity correlators in (A6) and (A7).

b. 2D blue state on a semi-infinite cylinder with generic boundary condition

We consider the Hamiltonian H_{blue} on a semi-infinite cylinder, i.e, with open boundary condition on the y direction. Let the y coordinate run from $-\infty$ to $\dots, k_0, k_0 + \frac{1}{2}$ with the top boundary on blue vertices. Now we trace out all the 2D d.o.f. except the top row at $y = k_0$ and $y = k_0 + \frac{1}{2}$ (we call the top rows again region A). Tracing out A^c gives

$$\text{Tr}_{A^c} (|\text{blue}\rangle \langle \text{blue}|) = \frac{2}{2^{|\Delta_{v_r} \cap A|}} \sum_{\substack{\{i_l\} \in \Delta_{v_r} \cap A, \\ s \text{ even}}} \left(Z_{i_1} \prod_{j_1 \in \text{Nb}(i_1)} Z_{j_1} \right) \dots \left(Z_{i_s} \prod_{j_s \in \text{Nb}(i_s)} Z_{j_s} \right) \prod CZ_{v_r, v_b} |+\rangle^{\otimes \Delta_{v_r}} |\phi\rangle^{\otimes \Delta_{v_b}} \quad (\text{A11a})$$

$$\langle \phi |^{\otimes \Delta_{v_b}} \langle + |^{\otimes \Delta_{v_r}} \prod CZ_{v_r, v_b} \left(Z_{i_1} \prod_{j_1 \in \text{Nb}(i_1)} Z_{j_1} \right) \dots \left(Z_{i_s} \prod_{j_s \in \text{Nb}(i_s)} Z_{j_s} \right) \equiv \bar{\rho}_{\text{blue}}^A, \quad (\text{A11b})$$

where $|\phi\rangle$ is an arbitrary dangling d.o.f. on the blue vertices. $\text{Nb}(i_l)$ denote the neighboring blue vertex to the red vertex i_l in A. It has a strong $\mathbb{Z}_2^{(r)} = \prod_i X_{i, k_0}$ symmetry. Stabilizers satisfy the following weak symmetry condition

$$Z_{i-\frac{1}{2}, k_0+\frac{1}{2}} X_{i, k_0} Z_{i+\frac{1}{2}, k_0+\frac{1}{2}} \bar{\rho}_{\text{blue}}^A Z_{i-\frac{1}{2}, k_0+\frac{1}{2}} X_{i, k_0} Z_{i+\frac{1}{2}, k_0+\frac{1}{2}} = \bar{\rho}_{\text{blue}}^A. \quad (\text{A12})$$

$\bar{\rho}_{\text{blue}}^A$ exhibits SWSSB of $\mathbb{Z}_2^{(r)}$ symmetry when $\langle \phi | Z | \phi \rangle \neq 0$.

c. Tracing the interface between 2D cluster state and 2D blue state on a torus

Now let us consider the two-dimensional state that constitutes an interface between the cluster state and the blue state, subject to periodic boundary conditions along y direction. We take the interface to lie along the lines $x = l + \frac{1}{2}$ and $x = L_x + \frac{1}{2}$. In this setting, after tracing out all bulk degrees of freedom except for the layers at $y = k$ and $y = k + \frac{1}{2}$, the resulting reduced density matrix is given by $\rho_{1D-SWSSB}^A$. This outcome is anticipated, since tracing out all bulk degrees of freedom except those at $y = k$ and $y = k + \frac{1}{2}$ yields the same reduced state, regardless of whether the initial state is the cluster state or the blue state with periodic boundary conditions.

d. Tracing the interface between 2D cluster state and 2D blue state on a cylinder with generic open boundary condition

Let us consider the two dimensional state that constitute an interface between the 2D cluster state and 2D blue state, subject to open boundary condition along the y direction. We take the boundary to lie at $y = k_0$ and $y = k_0 + \frac{1}{2}$. We take the interface to lie along the lines $x = l + \frac{1}{2}$ and $x = L_x + \frac{1}{2}$. After tracing out the bulk degrees of freedom except for the layers at $y = k_0$ and $y = k_0 + \frac{1}{2}$, the resulting reduced density matrix has SWSSB of $\mathbb{Z}_2^{(r)}$ symmetry.

3. Mixed state from 2D blue^{k₀;k₁} state

In this section, we look at the states obtained by tracing out the 2D blue^{k₀;k₁} state on a torus and on cylinder with generic boundary condition. The results are summarized in Table V.

a. 2D blue^{k₀;k₁} state on a torus

Now we trace out all the 2D d.o.f. except the row at $y = k_1$ and $y = k_1 + \frac{1}{2}$. Tracing out A^c gives

$$\begin{aligned} & \text{Tr}_{A^c} \left(\left| \text{blue}^{k_0; k_1} \right\rangle \left\langle \text{blue}^{k_0; k_1} \right| \right) \\ &= \frac{4}{2^{|\Delta_{v_b} \cap A| + |\Delta_{v_r} \cap A|}} \sum_{\substack{\{k_l\} \in \Delta_{v_b} \cap A, \\ t \text{ even} \\ \{i_l\} \in \Delta_{v_r} \cap A, \\ s \text{ even}}} Z_{k_1}^b \dots Z_{k_t}^b \times Z_{i_1}^r \dots Z_{i_s}^r \\ & \quad \prod_{v_b=(i+\frac{1}{2}, k_1+\frac{1}{2})} CZ_{v_b, v_b+(1,0)} |1\text{D-cluster}\rangle \langle 1\text{D-cluster}| \prod_{v_b=(i+\frac{1}{2}, k_1+\frac{1}{2})} CZ_{v_b, v_b+(1,0)} \\ & \quad \times Z_{i_1}^r \dots Z_{i_s}^r \times Z_{k_1}^b \dots Z_{k_t}^b \end{aligned} \quad (\text{A13a})$$

$$= \left[\prod_{v_b=(i+\frac{1}{2}, k_1+\frac{1}{2})} CZ_{v_b, v_b+(1,0)} \right] \rho_{1\text{D-SWSSB}}^A \left[\prod_{v_b=(i+\frac{1}{2}, k_1+\frac{1}{2})} CZ_{v_b, v_b+(1,0)} \right] = \rho_{1\text{D-SWSSB}}^A. \quad (\text{A13b})$$

This state was studied in (A1) and has strong $\mathbb{Z}_2^{(r)} \times \mathbb{Z}_2^{(b)}$ 0-form symmetry and weak emergent non-invertible $D^{(1)}$ symmetry. We verified that it is in the SWSSB phase regarding the $\mathbb{Z}_2^{(r)} \times \mathbb{Z}_2^{(b)}$ by computing the Rényi-2 correlator and the fidelity correlators in (A6) and (A7).

b. 2D blue^{k₀;k₁} on a semi-infinite cylinder with generic boundary condition

Now we consider the state blue^{k₀;k₁} with open boundary condition in y direction, with y values ranging from $-\infty$, ..., k_0 , $k_0 + \frac{1}{2}$, ..., k_1 , $k_1 + \frac{1}{2}$. We take $y = k_1$ and $y = k_1 + \frac{1}{2}$ as the region A and the rest as A^c . Tracing out the region A^c , we obtain the state

$$\text{Tr}_{A^c} \left(\left| \text{blue}^{k_0; k_1} \right\rangle \left\langle \text{blue}^{k_0; k_1} \right| \right) = \left[\prod_{v_b=(i+\frac{1}{2}, k_1+\frac{1}{2})} CZ_{v_b, v_b+(1,0)} \right] \bar{\rho}_{\text{blue}}^A \left[\prod_{v_b=(i+\frac{1}{2}, k_1+\frac{1}{2})} CZ_{v_b, v_b+(1,0)} \right] \equiv \bar{\rho}_{\text{blue}^{k_0; k_1}}^A. \quad (\text{A14})$$

with arbitrary dangling d.o.f. $|\phi\rangle$ on the vertices at $y = k_1 + \frac{1}{2}$ at the boundary.

This state has the weak stabilizers

$$Z_{i-\frac{1}{2}, k_1+\frac{1}{2}} X_{i, k_1} Z_{i+\frac{1}{2}, k_1+\frac{1}{2}} \bar{\rho}_{\text{blue}^{k_0; k_1}}^A Z_{i-\frac{1}{2}, k_1+\frac{1}{2}} X_{i, k_1} Z_{i+\frac{1}{2}, k_1+\frac{1}{2}} = \bar{\rho}_{\text{blue}^{k_0; k_1}}^A, \quad (\text{A15})$$

$\bar{\rho}_{\text{blue}^{k_0; k_1}}^A$ is in the SWSSB phase regarding the $\mathbb{Z}_2^{(r)}$ symmetry when $\langle \phi | Z | \phi \rangle \neq 0$.

c. Tracing the interface between 2D cluster state and 2D blue^{k₀;k₁} state on a torus

Now let us consider the two-dimensional state that constitutes an interface between the cluster state and the blue^{k₀;k₁} state, subject to periodic boundary conditions along y direction. We take the interface to lie along the lines $x = l + \frac{1}{2}$ and $x = L_x + \frac{1}{2}$. In this setting, after tracing out all bulk degrees of freedom except for the layers at $y = k$ and $y = k + \frac{1}{2}$, the resulting reduced density matrix is given by

$$\prod_{\substack{v_b=(i+\frac{1}{2}, k_1+\frac{1}{2}) \\ l \leq i < L_x}} CZ_{v_b, v_b+(1,0)} \rho_{1\text{D-SWSSB}}^A \prod_{\substack{v_b=(i+\frac{1}{2}, k_1+\frac{1}{2}) \\ l \leq i < L_x}} CZ_{v_b, v_b+(1,0)}. \quad (\text{A16})$$

This outcome is anticipated, since tracing out all bulk degrees of freedom except those at $y = k$ and $y = k + \frac{1}{2}$ yields the same reduced state, regardless of whether the initial state is the cluster state or the blue state with periodic boundary conditions and we have an extra decoration by the CZ gate to account for the blue^{k₀;k₁} state.

Boundary condition in 2D	Strong symmetries	Weak symmetries	Phase
Periodic in x and y	$\mathbb{Z}_2^{(r)} = \prod_i X_{i,0}$, $\mathbb{Z}_2^{(b)} = \prod_i X_{i+\frac{1}{2},\frac{1}{2}}$	$D^{(1)}$ $Z_{i,k} X_{i+\frac{1}{2},k+\frac{1}{2}} Z_{i+1,k}$ $Z_{i-\frac{1}{2},k+\frac{1}{2}} X_{i,k} Z_{i+\frac{1}{2},k+\frac{1}{2}}$	SWSSB of $\mathbb{Z}_2^{(r)}$ and $\mathbb{Z}_2^{(b)}$
Periodic in x and open in y with boundary at $y = k_0 + \frac{1}{2} = \frac{1}{2}$	$\mathbb{Z}_2^{(r)} = \prod_i X_{i,0}$	$Z_{i-\frac{1}{2},\frac{1}{2}} X_{i,0} Z_{i+\frac{1}{2},\frac{1}{2}}$	SWSSB of $\mathbb{Z}_2^{(r)}$
Periodic in y and open in x with boundary at $x = l + \frac{1}{2}$ and $x = L_x + \frac{1}{2}$	-	$\mathbb{Z}_2^{(r)} = Z_{l+\frac{1}{2},k+\frac{1}{2}} \prod_{i=l+1}^{L_x} X_{i,k} Z_{L_x+\frac{1}{2},k+\frac{1}{2}}$ $Z_{i-\frac{1}{2},k+\frac{1}{2}} X_{i,k} Z_{i+\frac{1}{2},k+\frac{1}{2}} (i = l+1, \dots, L_x)$ $Z_{i,k} X_{i+\frac{1}{2},k+\frac{1}{2}} Z_{i+1,k} (i = l+1, \dots, L_x - 1)$	$\mathbb{Z}_2^{(r)}$ is explicitly broken to weak symmetry $\mathbb{Z}_2^{(b)}$ is explicitly broken to nothing
Open in x and open in y with boundary at $y = k_0 + \frac{1}{2} = \frac{1}{2}$ and $x = l + \frac{1}{2}, L_x + \frac{1}{2}$	-	$\mathbb{Z}_2^{(r)} = Z_{l+\frac{1}{2},\frac{1}{2}} \prod_{i=l+1}^{L_x} X_{i,0} Z_{L_x+\frac{1}{2},\frac{1}{2}}$ $Z_{i-\frac{1}{2},\frac{1}{2}} X_{i,0} Z_{i+\frac{1}{2},\frac{1}{2}} (i = l+1, \dots, L_x)$	$\mathbb{Z}_2^{(r)}$ is explicitly broken to weak symmetry

TABLE I: A table illustrating the properties of the state after tracing out the cluster state in the 2D with arbitrary dangling d.o.f. on boundaries.

Boundary condition in 2D	Strong symmetries	Weak symmetries	Phase
Periodic in x and open in y with boundary at $y = k_0 + \frac{1}{2} = \frac{1}{2}$	$\mathbb{Z}_2^{(r)} = \prod_i X_{i,0}$ $\mathbb{Z}_2^{(b)} = \prod_i X_{i+\frac{1}{2},\frac{1}{2}}$ $D^{(1)}$ $Z_{i,k} X_{i+\frac{1}{2},k+\frac{1}{2}} Z_{i+1,k}$	$Z_{i-\frac{1}{2},k+\frac{1}{2}} X_{i,k} Z_{i+\frac{1}{2},k+\frac{1}{2}}$	SWSSB of $\mathbb{Z}_2^{(r)}$ Double ASPT
Periodic in y and open in x with boundary at $x = l + \frac{1}{2}$ and $x = L_x + \frac{1}{2}$	$\mathbb{Z}_2^{(b)} = \prod_{i=l}^{L_x} X_{i+\frac{1}{2},k+\frac{1}{2}}$	$\mathbb{Z}_2^{(r)} = Z_{l+\frac{1}{2},k+\frac{1}{2}} \prod_{i=l+1}^{L_x} X_{i,k} Z_{L_x+\frac{1}{2},k+\frac{1}{2}}$ $Z_{i-\frac{1}{2},k+\frac{1}{2}} X_{i,k} Z_{i+\frac{1}{2},k+\frac{1}{2}} (i = l+1, \dots, L_x)$ $Z_{i,k} X_{i+\frac{1}{2},k+\frac{1}{2}} Z_{i+1,k} (i = l+1, \dots, L_x - 1)$ $X_{l+\frac{1}{2}} Z_{l+1,k}, X_{L_x+\frac{1}{2},k+\frac{1}{2}} Z_{L_x,k}$	$\mathbb{Z}_2^{(r)}$ is explicitly broken to weak symmetry
Open in x and open in y with boundary at $y = k_0 + \frac{1}{2} = \frac{1}{2}$ and $x = l + \frac{1}{2}, L_x + \frac{1}{2}$	$\mathbb{Z}_2^{(b)} = \prod_{i=l}^{L_x} X_{i+\frac{1}{2},\frac{1}{2}}$ $Z_{i,0} X_{i+\frac{1}{2},\frac{1}{2}} Z_{i+1,0}$ $(i = l+1, \dots, L_x - 1)$ $X_{l+\frac{1}{2}} Z_{l+1,0}, X_{L_x+\frac{1}{2},\frac{1}{2}} Z_{L_x,0}$	$\mathbb{Z}_2^{(r)} = Z_{l+\frac{1}{2},\frac{1}{2}} \prod_{i=l+1}^{L_x} X_{i,0} Z_{L_x+\frac{1}{2},\frac{1}{2}}$ $Z_{i-\frac{1}{2},\frac{1}{2}} X_{i,0} Z_{i+\frac{1}{2},\frac{1}{2}} (i = l+1, \dots, L_x)$	mSPT

TABLE II: A table illustrating the properties of the state after tracing out the cluster state in the 2D with the dangling d.o.f. set to $|+\rangle$ state.

Boundary condition in 2D	Strong symmetries	Weak symmetries	Phase
Periodic in x and y	$\mathbb{Z}_2^{(r)} = \prod_i X_{i,k}$, $\mathbb{Z}_2^{(b)} = \prod_i X_{i+\frac{1}{2},k+\frac{1}{2}}$	$Z_{i,k} X_{i+\frac{1}{2},k+\frac{1}{2}} Z_{i+1,k}$ $Z_{i-\frac{1}{2},k+\frac{1}{2}} X_{i,k} Z_{i+\frac{1}{2},k+\frac{1}{2}}$ $D^{(1)}$	SWSSB of $\mathbb{Z}_2^{(b)}$ and $\mathbb{Z}_2^{(r)}$
Periodic in y and open in x with boundary at $x = l + \frac{1}{2}, L_x + \frac{1}{2}$	-	$Z_{i-\frac{1}{2},k+\frac{1}{2}} X_{i,k} Z_{i+\frac{1}{2},k+\frac{1}{2}} (i = l+1, \dots, L_x)$ $Z_{i,k} X_{i+\frac{1}{2},k+\frac{1}{2}} Z_{i+1,k} (i = l+1, \dots, L_x - 1)$ $\mathbb{Z}_2^{(r)} = Z_{l+\frac{1}{2}} \prod_{i=l+1}^{L_x} X_{i,k} Z_{L_x+\frac{1}{2},k+\frac{1}{2}}$	$\mathbb{Z}_2^{(r)}$ is explicitly broken to weak symmetry $\mathbb{Z}_2^{(b)}$ is explicitly broken to nothing
Periodic in x and open in y with boundary at $y = k_0 + \frac{1}{2} = \frac{1}{2}$	$\mathbb{Z}_2^{(r)} = \prod_i X_{i,0}$	$Z_{i-\frac{1}{2},k+\frac{1}{2}} X_{i,k} Z_{i+\frac{1}{2},k+\frac{1}{2}}$	SWSSB of $\mathbb{Z}_2^{(r)}$
Open in x and open in y with boundary at $y = k_0 + \frac{1}{2} = \frac{1}{2}$ and $x = l + \frac{1}{2}, L_x + \frac{1}{2}$	-	$\mathbb{Z}_2^{(r)} = Z_{\frac{1}{2},\frac{1}{2}} \prod_{i=1}^{l-1} X_{i,0} Z_{l-\frac{1}{2},\frac{1}{2}}$ $Z_{i-\frac{1}{2},k+\frac{1}{2}} X_{i,k} Z_{i+\frac{1}{2},k+\frac{1}{2}} (i = l+1, \dots, L_x)$	$\mathbb{Z}_2^{(r)}$ is explicitly broken to weak symmetry

TABLE III: A table illustrating the properties of the state after tracing out the blue state in the 2D with arbitrary d.o.f. at the boundary.

d. *Tracing the interface between 2D cluster state and 2D blue^{k₀:k₁} state on a cylinder with generic open boundary condition*

Now let us consider an interface between the 2D cluster state and the 2D blue^{k₀:k₁} state, subject to open boundary conditions along y direction. As in the previous case, the d.o.f. at $y = k_0 + \frac{1}{2}$ are arbitrary and we call it $|\phi\rangle$. For this generic boundary condition, the resulting state after tracing the bulk d.o.f is in the SWSSB phase of $\mathbb{Z}_2^{(r)}$

Boundary condition in 2D	Strong symmetries	Weak symmetries	Phase
Periodic in x and open in y with boundary at $y = k_0 + \frac{1}{2} = \frac{1}{2}$	$\mathbb{Z}_2^{(r)} = \prod_i X_{i,0}$ $\mathbb{Z}_2^{(b)} = \prod_i X_{i+\frac{1}{2},\frac{1}{2}}$ $D^{(1)}$	$Z_{i-\frac{1}{2},\frac{1}{2}} X_{i,0} Z_{i+\frac{1}{2},\frac{1}{2}}$ $Z_{i,0} X_{i+\frac{1}{2},\frac{1}{2}} Z_{i+1,0}$	SWSSB of $\mathbb{Z}_2^{(r)}$ Double ASPT
Periodic in y and open in x with boundary at $x = l + \frac{1}{2}, L_x + \frac{1}{2}$	-	$Z_{i-\frac{1}{2},k+\frac{1}{2}} X_{i,k} Z_{i+\frac{1}{2},k+\frac{1}{2}} \quad (i = l+1, \dots, L_x)$ $Z_{i,k} X_{i+\frac{1}{2},k+\frac{1}{2}} Z_{i+1,k} \quad (i = l+1, \dots, L_x - 1)$ $X_{l+\frac{1}{2},k+\frac{1}{2}} Z_{l+1,k}, \quad Z_{L_x,k} X_{L_x+\frac{1}{2},k+\frac{1}{2}}$ $\mathbb{Z}_2^{(r)} = Z_{l+\frac{1}{2}} \prod_{i=l+1}^{L_x} X_{i,k} Z_{L_x+\frac{1}{2},k+\frac{1}{2}}$ $\mathbb{Z}_2^{(b)} = \prod_{i=l}^{L_x} X_{i+\frac{1}{2},k+\frac{1}{2}}$	$\mathbb{Z}_2^{(r)}$ and $\mathbb{Z}_2^{(b)}$ is explicitly broken to weak symmetry
Open in x and open in y with boundary at $y = k_0 + \frac{1}{2} = \frac{1}{2}$ and $x = l + \frac{1}{2}, L_x + \frac{1}{2}$	$Z_{i-\frac{1}{2},\frac{1}{2}} Y_{i,0} X_{i+\frac{1}{2},\frac{1}{2}} Y_{i+1,0} Z_{i+\frac{1}{2},\frac{1}{2}}$ $(i = l+1, \dots, L_x - 1)$	$\mathbb{Z}_2^{(r)} = Z_{l+\frac{1}{2},\frac{1}{2}} \prod_{i=l+1}^{L_x} X_{i,0} Z_{L_x+\frac{1}{2},\frac{1}{2}}$ $\mathbb{Z}_2^{(b)} = \prod_{i=l}^{L_x} X_{i+\frac{1}{2},\frac{1}{2}}$ $Z_{i,0} X_{i+\frac{1}{2},\frac{1}{2}} Z_{i+1,0} \quad (i = l+1, \dots, L_x - 1)$ $Z_{i-\frac{1}{2},\frac{1}{2}} X_{i,0} Z_{i+\frac{1}{2},\frac{1}{2}} \quad (i = l+1, \dots, L_x)$ $X_{l+\frac{1}{2},\frac{1}{2}} Z_{l+1,0} \quad X_{L_x+\frac{1}{2},\frac{1}{2}} Z_{L_x,0}$	$\mathbb{Z}_2^{(r)}$ and $\mathbb{Z}_2^{(b)}$ is explicitly broken to weak symmetry

TABLE IV: A table illustrating the properties of the state after tracing out the blue state in the 2D with the dangling d.o.f. set to $|+\rangle$ state.

Boundary condition in 2D	Strong symmetries	Weak symmetries	Phase
Periodic in x and y	$\mathbb{Z}_2^{(r)} = \prod_i X_{i,k}$, $\mathbb{Z}_2^{(b)} = \prod_i X_{i+\frac{1}{2},k+\frac{1}{2}}$	$D^{(1)}$ $Z_{i,k} X_{i+\frac{1}{2},k+\frac{1}{2}} Z_{i+1,k}$ $Z_{i-\frac{1}{2},k+\frac{1}{2}} X_{i,k} Z_{i+\frac{1}{2},k+\frac{1}{2}}$	SWSSB of $\mathbb{Z}_2^{(r)}$ and $\mathbb{Z}_2^{(b)}$
Periodic in x and open in y with boundary at $y = k_1 + \frac{1}{2} = \frac{1}{2}$	$\mathbb{Z}_2^{(r)} = \prod_i X_{i,0}$	$Z_{i-\frac{1}{2},k+\frac{1}{2}} X_{i,k} Z_{i+\frac{1}{2},k+\frac{1}{2}}$	SWSSB of $\mathbb{Z}_2^{(r)}$
Periodic in y and open in x with boundary at $x = l + \frac{1}{2}, L_x + \frac{1}{2}$	-	$Z_{i-\frac{1}{2},k+\frac{1}{2}} X_{i,k} Z_{i+\frac{1}{2},k+\frac{1}{2}} \quad (i = l+1, \dots, L_x)$ $Z_{i-\frac{1}{2},k+\frac{1}{2}} Z_{i,k} X_{i+\frac{1}{2},k+\frac{1}{2}} Z_{i+1,k} Z_{i+\frac{3}{2},k+\frac{1}{2}}$ $(i = l+1, \dots, L_x - 1)$ $\mathbb{Z}_2^{(r)} = Z_{l+\frac{1}{2},k+\frac{1}{2}} \prod_{i=l+1}^{L_x} X_{i,k} Z_{L_x+\frac{1}{2},k+\frac{1}{2}}$ $\mathbb{Z}_2^{(b)} = Z_{l+\frac{1}{2},k+\frac{1}{2}} Z_{l+1,k} Y_{l+\frac{3}{2},k+\frac{1}{2}} \prod_{i=l+2}^{L_x-2} X_{i+\frac{1}{2},k+\frac{1}{2}}$ $\times Y_{L_x-\frac{1}{2},k+\frac{1}{2}} Z_{L_x,k} Z_{L_x+\frac{1}{2},k+\frac{1}{2}}$	$\mathbb{Z}_2^{(r)}$ and $\mathbb{Z}_2^{(b)}$ is explicitly broken to weak symmetry
Open in x and open in y with boundary at $y = k_1 + \frac{1}{2} = \frac{1}{2}$ and $x = l + \frac{1}{2}, L_x + \frac{1}{2}$	-	$\mathbb{Z}_2^{(r)} = Z_{\frac{1}{2},\frac{1}{2}} \prod_{i=1}^{l-1} X_{i,0} Z_{l-\frac{1}{2},\frac{1}{2}}$ $Z_{i-\frac{1}{2},\frac{1}{2}} X_{i,0} Z_{i+\frac{1}{2},\frac{1}{2}} \quad (i = l+1, \dots, L_x)$	$\mathbb{Z}_2^{(r)}$ is explicitly broken to weak symmetry

TABLE V: A table illustrating the properties of the state after tracing out the blue $k_0; k_1$ state in the 2D with arbitrary dangling d.o.f.

symmetry. This is expected since tracing individually the two states results in SWSSB of $\mathbb{Z}_2^{(r)}$ and does not possess the non-invertible symmetry $D^{(1)}$.

B. A symmetric interface between two DASPTs

In this appendix, we consider an interface between two DASPTs and show that that interface can be made symmetric under $\mathbb{Z}_2^{(r)} \times \mathbb{Z}_2^{(b)}$ and $D^{(1)}$. The two DASPTs are

$$\rho_{1\text{D-DASPT}} = \prod_i \frac{1 + Z_{i-1,k_0} X_{i+\frac{1}{2},k_0+\frac{1}{2}} Z_{i+1,k_0}}{2} \times \left(\frac{1 + \prod_i X_{i,k_0}}{2^{L_x}} \right) \quad (\text{B1a})$$

$$\rho_{1\text{D-DASPT}'} = \prod_i \frac{1 + Z_{i-\frac{1}{2},k_0+\frac{1}{2}} X_{i,k_0} Z_{i+\frac{1}{2},k_0+\frac{1}{2}}}{2} \times \left(\frac{1 + \prod_i X_{i+\frac{1}{2},k_0+\frac{1}{2}}}{2^{L_x}} \right). \quad (\text{B1b})$$

Boundary condition in 2D	Strong symmetries	Weak symmetries	Phase
Periodic in x and open in y with boundary at $y = k_1 + \frac{1}{2} = \frac{1}{2}$	$\mathbb{Z}_2^{(r)} = \prod_i X_{i,0}$ $\mathbb{Z}_2^{(b)} = \prod_i X_{i+\frac{1}{2},\frac{1}{2}}$ $Y_{i,0}X_{i+\frac{1}{2},\frac{1}{2}}Y_{i+1,0}$	$Z_{i-\frac{1}{2},\frac{1}{2}}X_{i,0}Z_{i+\frac{1}{2},\frac{1}{2}}$ $Z_{i-\frac{1}{2},\frac{1}{2}}Z_{i,0}X_{i+\frac{1}{2},\frac{1}{2}}Z_{i+1,0}Z_{i+\frac{3}{2},\frac{1}{2}}$	SWSSB of $\mathbb{Z}_2^{(r)}$
Periodic in y and open in x with boundary at $x = l + \frac{1}{2}, L_x + \frac{1}{2}$	-	$Z_{i-\frac{1}{2},k+\frac{1}{2}}X_{i,k}Z_{i+\frac{1}{2},k+\frac{1}{2}} \quad (i = l+1, \dots, L_x)$ $Z_{i-\frac{1}{2},k+\frac{1}{2}}Z_{i,k}X_{i+\frac{1}{2},k+\frac{1}{2}}Z_{i+1,k}Z_{i+\frac{3}{2},k+\frac{1}{2}} \quad (i = l+1, \dots, L_x-1)$ $X_{l+\frac{1}{2},k+\frac{1}{2}}Z_{l+1,k}Z_{l+\frac{3}{2},k+\frac{1}{2}}$ $X_{L_x+\frac{1}{2},k+\frac{1}{2}}Z_{L_x,k}Z_{L_x-\frac{1}{2},k+\frac{1}{2}}$ $\mathbb{Z}_2^{(r)} = Z_{l+\frac{1}{2},k+\frac{1}{2}} \prod_{i=l+1}^{L_x} X_{i,k}Z_{L_x+\frac{1}{2},k+\frac{1}{2}}$ $\mathbb{Z}_2^{(b)} = Y_{l+\frac{1}{2},k+\frac{1}{2}} \prod_{i=l+1}^{L_x-1} X_{i+\frac{1}{2},k+\frac{1}{2}}Y_{L_x+\frac{1}{2},k+\frac{1}{2}}$	$\mathbb{Z}_2^{(r)}$ and $\mathbb{Z}_2^{(b)}$ is explicitly broken to weak symmetry
Open in x and open in y with boundary at $y = k_1 + \frac{1}{2} = \frac{1}{2}$ and $x = l + \frac{1}{2}, L_x + \frac{1}{2}$	$Y_{i,0}X_{i+\frac{1}{2},\frac{1}{2}}Y_{i+1,0}$ $(i = l+1, \dots, L_x-1)$	$Z_{i-\frac{1}{2},\frac{1}{2}}X_{i,0}Z_{i+\frac{1}{2},\frac{1}{2}} \quad (i = l+1, \dots, L_x)$ $Z_{i-\frac{1}{2},\frac{1}{2}}Z_{i,0}X_{i+\frac{1}{2},\frac{1}{2}}Z_{i+1,0}Z_{i+\frac{3}{2},\frac{1}{2}} \quad (i = l+1, \dots, L_x-1)$ $X_{l+\frac{1}{2},\frac{1}{2}}Z_{l+1,0}Z_{l+\frac{3}{2},\frac{1}{2}}$ $X_{L_x+\frac{1}{2},\frac{1}{2}}Z_{L_x,0}Z_{L_x-\frac{1}{2},\frac{1}{2}}$ $\mathbb{Z}_2^{(r)} = Z_{l+\frac{1}{2},\frac{1}{2}} \prod_{i=l+1}^{L_x} X_{i,0}Z_{L_x+\frac{1}{2},\frac{1}{2}}$ $\mathbb{Z}_2^{(b)} = Y_{l+\frac{1}{2},\frac{1}{2}} \prod_{i=l+1}^{L_x-1} X_{i+\frac{1}{2},\frac{1}{2}}Y_{L_x+\frac{1}{2},\frac{1}{2}}$	$\mathbb{Z}_2^{(r)}$ and $\mathbb{Z}_2^{(b)}$ is explicitly broken to weak symmetry

TABLE VI: A table illustrating the properties of the state after tracing out the blue $^{k_0;k_1}$ state in the 2D with dangling d.o.f. set to $|+\rangle$ state.

Boundary condition in 2D	Strong symmetries	SWSSB	Weak symmetries
Periodic in y with interface at $x = l + \frac{1}{2}, L_x + \frac{1}{2}$	$\mathbb{Z}_2^{(r)} \times \mathbb{Z}_2^{(b)}$	$\mathbb{Z}_2^{(r)} \times \mathbb{Z}_2^{(b)}$	$D^{(1)}$
Open in y with interface at $x = l + \frac{1}{2}, L_x + \frac{1}{2}$	$\mathbb{Z}_2^{(r)} \times \mathbb{Z}_2^{(b)}, D^{(1)}$	$\mathbb{Z}_2^{(r)}$	

TABLE VII: A table illustrating the properties of interface between 2D cluster state and 2D blue state. Vertex d.o.f. at the interface is set to $|+\rangle$.

Boundary condition in 2D	Strong symmetries	SWSSB	Weak symmetries
Periodic in y with interface at $x = l + \frac{1}{2}, L_x + \frac{1}{2}$	$\mathbb{Z}_2^{(r)} \times \mathbb{Z}_2^{(b)}$	$\mathbb{Z}_2^{(r)} \times \mathbb{Z}_2^{(b)}$	$D^{(1)}$
Open in y with interface at $x = l + \frac{1}{2}, L_x + \frac{1}{2}$	$\mathbb{Z}_2^{(r)} \times \mathbb{Z}_2^{(b)}$	$\mathbb{Z}_2^{(r)}$	

TABLE VIII: A table illustrating the properties of interface between 2D cluster state and 2D blue $^{k_0;k_1}$ state. Vertex d.o.f. at the interface is set to $|+\rangle$.

Now we consider an interface between the two with interface located at $(l + \frac{1}{2}, k_0 + \frac{1}{2})$ and $(L_x + \frac{1}{2}, k_0 + \frac{1}{2})$. As before we assume periodic boundary condition $L_x + 1 \equiv 1$. The interface state is obtained by truncating the two DASPTs

$$\rho_{1D\text{-DASPT}|1D\text{-DASPT}'} = \prod_{i=1}^l \frac{1 + Z_{i-\frac{1}{2},k_0+\frac{1}{2}}X_{i,k_0}Z_{i+\frac{1}{2},k_0+\frac{1}{2}}}{2} \times \frac{1 + Z_{1,k_0} \prod_{i=1}^{l-1} X_{i+\frac{1}{2},k_0+\frac{1}{2}}Z_{l,k_0}}{2^{l-1}}$$

$$\prod_{i=l+1}^{L_x-1} \frac{1 + Z_{i,k_0}X_{i+\frac{1}{2},k_0+\frac{1}{2}}Z_{i+1,k_0}}{2} \times \frac{1 + Z_{l+\frac{1}{2},k_0+\frac{1}{2}} \prod_{i=l+1}^{L_x} X_{i,k_0}Z_{L_x+\frac{1}{2},k_0+\frac{1}{2}}}{2^{L_x-l}}. \quad (\text{B2})$$

Acting with the invertible symmetry operators

$$\prod_i X_{i,k_0} \rho_{1\text{D-DASPT}|1\text{D-DASPT}'} = \rho_{1\text{D-DASPT}|1\text{D-DASPT}'} \quad (\text{B3})$$

$$\prod_i X_{i+\frac{1}{2},k_0+\frac{1}{2}} \rho_{1\text{D-DASPT}|1\text{D-DASPT}'} = Z_{l,k_0} X_{l+\frac{1}{2},k_0+\frac{1}{2}} Z_{l+1,k_0} \times Z_{L_x,k_0} X_{L_x+\frac{1}{2},k_0+\frac{1}{2}} Z_{1,k_0} \rho_{1\text{D-DASPT}|1\text{D-DASPT}'} \cdot \quad (\text{B4})$$

To make the interface state symmetric under the invertible symmetries, we can add the projectors and define

$$\tilde{\rho}_{1\text{D-DASPT}|1\text{D-DASPT}'} = \frac{1 + Z_{l,k_0} X_{l+\frac{1}{2},k_0+\frac{1}{2}} Z_{l+1,k_0}}{2} \times \frac{1 + Z_{L_x,k_0} X_{L_x+\frac{1}{2},k_0+\frac{1}{2}} Z_{1,k_0}}{2} \rho_{1\text{D-DASPT}|1\text{D-DASPT}'} \cdot \quad (\text{B5})$$

It is a straightforward exercise to check that $\tilde{\rho}_{1\text{D-DASPT}|1\text{D-DASPT}'}$ has strong $D^{(1)}$ symmetry in addition to the strong $\mathbb{Z}_2^{(r)} \times \mathbb{Z}_2^{(b)}$.

C. Details on the strong symmetry of $\rho_{\text{blue}}^{\text{A}}$

Let us consider the action of $D^{(1)}$ on $\rho_{\text{blue}}^{\text{A}}$

$$\begin{aligned} D^{(1)} \rho_{\text{blue}}^{\text{A}} &= D^{(1)} \frac{2}{2^{|\Delta_{v_r} \cap \text{A}|}} \sum_{\substack{\{i_l\} \in \Delta_{v_r} \cap \text{A}, \\ s \text{ even}}} \left(Z_{i_1} \prod_{j_1 \in \text{Nb}(i_1)} Z_{j_1} \right) \dots \left(Z_{i_s} \prod_{j_s \in \text{Nb}(i_s)} Z_{j_s} \right) \prod CZ_{v_r, v_b} |+\rangle^{\otimes \Delta_{v_r}} |+\rangle^{\otimes \Delta_{v_b}} \\ &\quad \langle + |^{\otimes \Delta_{v_b}} \langle + |^{\otimes \Delta_{v_r}} \prod CZ_{v_r, v_b} \left(Z_{i_1} \prod_{j_1 \in \text{Nb}(i_1)} Z_{j_1} \right) \dots \left(Z_{i_s} \prod_{j_s \in \text{Nb}(i_s)} Z_{j_s} \right) \\ &= \frac{2}{2^{|\Delta_{v_r} \cap \text{A}|}} \sum_{\substack{\{i_l\} \in \Delta_{v_r} \cap \text{A}, \\ s \text{ even}}} X_{i_1} \dots X_{i_s} D^{(1)} Z_{i_1} \dots Z_{i_s} \prod CZ_{v_r, v_b} |+\rangle^{\otimes \Delta_{v_r}} |+\rangle^{\otimes \Delta_{v_b}} \\ &\quad \langle + |^{\otimes \Delta_{v_b}} \langle + |^{\otimes \Delta_{v_r}} \prod CZ_{v_r, v_b} \left(Z_{i_1} \prod_{j_1 \in \text{Nb}(i_1)} Z_{j_1} \right) \dots \left(Z_{i_s} \prod_{j_s \in \text{Nb}(i_s)} Z_{j_s} \right) \\ &= \frac{2}{2^{|\Delta_{v_r} \cap \text{A}|}} \sum_{\substack{\{i_l\} \in \Delta_{v_r} \cap \text{A}, \\ s \text{ even}}} X_{i_1} \dots X_{i_s} X_{k_1} \dots X_{k_r} D^{(1)} \prod CZ_{v_r, v_b} |+\rangle^{\otimes \Delta_{v_r}} |+\rangle^{\otimes \Delta_{v_b}} \\ &\quad \langle + |^{\otimes \Delta_{v_b}} \langle + |^{\otimes \Delta_{v_r}} \prod CZ_{v_r, v_b} \left(Z_{i_1} \prod_{j_1 \in \text{Nb}(i_1)} Z_{j_1} \right) \dots \left(Z_{i_s} \prod_{j_s \in \text{Nb}(i_s)} Z_{j_s} \right) \quad (\text{C1}) \\ &= \frac{2}{2^{|\Delta_{v_r} \cap \text{A}|}} \sum_{\substack{\{i_l\} \in \Delta_{v_r} \cap \text{A}, \\ s \text{ even}}} X_{i_1} \dots X_{i_s} Z_{i_1} \dots Z_{i_s} 2 \prod CZ_{v_r, v_b} |+\rangle^{\otimes \Delta_{v_r}} |+\rangle^{\otimes \Delta_{v_b}} \\ &\quad \langle + |^{\otimes \Delta_{v_b}} \langle + |^{\otimes \Delta_{v_r}} \prod CZ_{v_r, v_b} \left(Z_{i_1} \prod_{j_1 \in \text{Nb}(i_1)} Z_{j_1} \right) \dots \left(Z_{i_s} \prod_{j_s \in \text{Nb}(i_s)} Z_{j_s} \right) \\ &= \frac{4}{2^{|\Delta_{v_r} \cap \text{A}|}} \sum_{\substack{\{i_l\} \in \Delta_{v_r} \cap \text{A}, \\ s \text{ even}}} \left(Z_{i_1} \prod_{j_1 \in \text{Nb}(i_1)} Z_{j_1} \right) \dots \left(Z_{i_s} \prod_{j_s \in \text{Nb}(i_s)} Z_{j_s} \right) \prod CZ_{v_r, v_b} |+\rangle^{\otimes \Delta_{v_r}} |+\rangle^{\otimes \Delta_{v_b}} \\ &\quad \langle + |^{\otimes \Delta_{v_b}} \langle + |^{\otimes \Delta_{v_r}} \prod CZ_{v_r, v_b} \left(Z_{i_1} \prod_{j_1 \in \text{Nb}(i_1)} Z_{j_1} \right) \dots \left(Z_{i_s} \prod_{j_s \in \text{Nb}(i_s)} Z_{j_s} \right) \\ &= 2 \rho_{\text{blue}}^{\text{A}} \end{aligned}$$

In the third equality, we converted product of Z operators on the red sublattice to product of X operators on the blue sublattice. In the fourth line, we used the fact that $D^{(1)} |\text{cluster}\rangle = 2 |\text{cluster}\rangle$ and converted back the product of

X operators on the blue sublattice to product of Z operators on red sublattice. Finally, in the fifth line, we converted back the product of X operators on the red sublattice to product of Z operators on the blue sublattice.

D. Other choices of interface cuts

1. Other choices of interface cuts between ρ_{trivial} and $\rho_{\text{1D-DASPT}}$

a. Interface cut at (l, k_0) and (L_x, k_0)

Let us consider an interface cut passing through (l, k_0) and (L_x, k_0) . The interface state is

$$\rho_{\text{trivial|1D-DASPT}}^{(1)} = \prod_{i=1}^{l-1} \frac{(1 + X_{i,k_0})}{2} \prod_{i=0}^{l-1} \frac{(1 + X_{i+\frac{1}{2},k_0+\frac{1}{2}})}{2} \prod_{i=l}^{L_x-1} \frac{(1 + Z_{i,k_0} X_{i+\frac{1}{2},k_0+\frac{1}{2}} Z_{i+1,k_0})}{2} \left(\frac{1 + \prod_{i=l}^{L_x} X_{i,k_0}}{2^{L_x-l+1}} \right). \quad (\text{D1})$$

Now we apply the symmetries on this state

$$\prod_i X_{i,k_0} \rho_{\text{trivial|1D-DASPT}}^{(1)} = \rho_{\text{trivial|1D-DASPT}}^{(1)} \quad (\text{D2a})$$

$$\prod_i X_{i+\frac{1}{2},k_0+\frac{1}{2}} \rho_{\text{trivial|1D-DASPT}}^{(1)} = Z_{l,k_0} Z_{L_x,k_0} \rho_{\text{trivial|1D-DASPT}}^{(1)}. \quad (\text{D2b})$$

Now if we add the projectors $Z_{l,k_0} = \pm 1$ and $Z_{L_x,k_0} = \pm 1$, then that would explicitly break the symmetry $\prod_i X_{i,k_0}$ to nothing.

b. Interface cut at $(l + \frac{1}{2}, k_0 + \frac{1}{2})$ and (L_x, k_0)

Now let us consider an interface cut at $(l + \frac{1}{2}, k_0 + \frac{1}{2})$ and (L_x, k_0) . The interface state is

$$\rho_{\text{trivial|1D-DASPT}}^{(2)} = \prod_{i=1}^l \frac{(1 + X_{i,k_0})}{2} \prod_{i=0}^{l-1} \frac{(1 + X_{i+\frac{1}{2},k_0+\frac{1}{2}})}{2} \prod_{i=l+1}^{L_x-1} \frac{(1 + Z_{i,k_0} X_{i+\frac{1}{2},k_0+\frac{1}{2}} Z_{i+1,k_0})}{2} \left(\frac{1 + Z_{l+\frac{1}{2},k_0+\frac{1}{2}} \prod_{i=l+1}^{L_x} X_{i,k_0}}{2^{L_x-l}} \right). \quad (\text{D3})$$

Now we apply the symmetries on this state

$$\prod_i X_{i,k_0} \rho_{\text{trivial|1D-DASPT}}^{(2)} = Z_{l+\frac{1}{2},k_0+\frac{1}{2}} \rho_{\text{trivial|1D-DASPT}}^{(2)} \quad (\text{D4a})$$

$$\prod_i X_{i+\frac{1}{2},k_0+\frac{1}{2}} \rho_{\text{trivial|1D-DASPT}}^{(2)} = X_{l+\frac{1}{2},k_0+\frac{1}{2}} Z_{l+1,k_0} Z_{L_x,k_0} \rho_{\text{trivial|1D-DASPT}}^{(2)}. \quad (\text{D4b})$$

It is clear that if we try to preserve one of the symmetry by adding a projector onto the interface state, then the other symmetry is explicitly broken to nothing. Interface cut at (l, k_0) and $(L_x + \frac{1}{2}, k_0 + \frac{1}{2})$ is similar to this case.

2. Other choices of interface cuts between $\rho_{\text{1D-DASPT}}$ and ρ_{blue}

a. Interface cut at (l, k_0) and (L_x, k_0)

Let us consider an interface cut passing through (l, k_0) and (L_x, k_0) . The interface state is

$$\rho_{\text{1D-DASPT|blue}}^{(1)} = \prod_{i=0}^{l-1} \frac{(1 + Z_{i,k_0} X_{i+\frac{1}{2},k_0+\frac{1}{2}} Z_{i+1,k_0})}{2} \prod_{i=l+1}^{L_x-2} \frac{(1 - Z_{i-\frac{1}{2},k_0+\frac{1}{2}} Y_{i,k_0} X_{i+\frac{1}{2},k_0} Y_{i+1,k_0} Z_{i+\frac{3}{2},k_0+\frac{1}{2}})}{2} \prod_i \frac{(1 + \prod_i X_{i,k_0})}{2^{L_x}} \quad (\text{D5})$$

Now we apply the symmetries on this state

$$\prod_i X_{i,k_0} \rho_{1\text{D-DASPT|blue}}^{(1)} = \rho_{1\text{D-DASPT|blue}}^{(1)} \quad (\text{D6a})$$

$$\prod_i X_{i+\frac{1}{2},k_0+\frac{1}{2}} \rho_{1\text{D-DASPT|blue}}^{(1)} = Z_{l,k_0} Y_{l+\frac{1}{2},k_0+\frac{1}{2}} Y_{l+1,k_0} Z_{l+\frac{3}{2},k_0+\frac{1}{2}} \times \\ Z_{L_x-\frac{3}{2},k_0+\frac{1}{2}} Y_{L_x-1,k_0} Y_{L_x-\frac{1}{2},k_0+\frac{1}{2}} Z_{L_x,k_0} \rho_{1\text{D-DASPT|blue}}^{(1)}. \quad (\text{D6b})$$

To make the state $\rho_{1\text{D-DASPT|blue}}^{(1)}$ symmetric under the invertible symmetries, we need to add the projectors $Z_{l,k_0} Y_{l+\frac{1}{2},k_0+\frac{1}{2}} Y_{l+1,k_0} Z_{l+\frac{3}{2},k_0+\frac{1}{2}} = \pm 1$ and $Z_{L_x-\frac{3}{2},k_0+\frac{1}{2}} Y_{L_x-1,k_0} Y_{L_x-\frac{1}{2},k_0+\frac{1}{2}} Z_{L_x,k_0} = \pm 1$. The state with $Z_{l,k_0} Y_{l+\frac{1}{2},k_0+\frac{1}{2}} Y_{l+1,k_0} Z_{l+\frac{3}{2},k_0+\frac{1}{2}} = -1$ and $Z_{L_x-\frac{3}{2},k_0+\frac{1}{2}} Y_{L_x-1,k_0} Y_{L_x-\frac{1}{2},k_0+\frac{1}{2}} Z_{L_x,k_0} = -1$ has a strong non-invertible symmetry $D^{(1)}$ and maybe indicating $\rho_{1\text{D-DASPT}}$ and ρ_{blue} are in the same phase with both invertible and non-invertible symmetries.

b. Interface cut at $(l + \frac{1}{2}, k_0 + \frac{1}{2})$ and (L_x, k_0)

Now let us consider an interface cut passing through $(l + \frac{1}{2}, k_0 + \frac{1}{2})$ and (L_x, k_0) . The interface state is

$$\rho_{1\text{D-DASPT|blue}}^{(2)} = \prod_{i=1}^{l-1} \frac{(1 + Z_{i,k_0} X_{i+\frac{1}{2},k_0+\frac{1}{2}} Z_{i+1,k_0})}{2} \prod_{i=l+1}^{L_x-2} \frac{(1 - Z_{i-\frac{1}{2},k_0+\frac{1}{2}} Y_{i,k_0} X_{i+\frac{1}{2},k_0} Y_{i+1,k_0} Z_{i+\frac{3}{2},k_0+\frac{1}{2}})}{2} \\ \times \frac{(1 + \prod_i X_{i,k_0})}{2^{L_x}} \quad (\text{D7})$$

Now we apply the symmetries on this state

$$\prod_i X_{i,k_0} \rho_{1\text{D-DASPT|blue}}^{(2)} = \rho_{1\text{D-DASPT|blue}}^{(2)} \quad (\text{D8a})$$

$$\prod_i X_{i+\frac{1}{2},k_0+\frac{1}{2}} \rho_{1\text{D-DASPT|blue}}^{(2)} = Z_{l,k_0} Y_{l+\frac{1}{2},k_0+\frac{1}{2}} Y_{l+1,k_0} Z_{l+\frac{3}{2},k_0+\frac{1}{2}} \times \\ Z_{L_x-\frac{3}{2},k_0+\frac{1}{2}} Y_{L_x-1,k_0} Y_{L_x-\frac{1}{2},k_0+\frac{1}{2}} Z_{L_x,k_0} \rho_{1\text{D-DASPT|blue}}^{(2)} \quad (\text{D8b})$$

To make the state $\rho_{1\text{D-DASPT|blue}}^{(2)}$ symmetric under the invertible symmetries, we add the projectors $Z_{l,k_0} Y_{l+\frac{1}{2},k_0+\frac{1}{2}} Y_{l+1,k_0} Z_{l+\frac{3}{2},k_0+\frac{1}{2}} = \pm 1$, and $Z_{L_x-\frac{3}{2},k_0+\frac{1}{2}} Y_{L_x-1,k_0} Y_{L_x-\frac{1}{2},k_0+\frac{1}{2}} Z_{L_x,k_0} = \pm 1$. The state with $Z_{l,k_0} Y_{l+\frac{1}{2},k_0+\frac{1}{2}} Y_{l+1,k_0} Z_{l+\frac{3}{2},k_0+\frac{1}{2}} = -1$ and $Z_{L_x-\frac{3}{2},k_0+\frac{1}{2}} Y_{L_x-1,k_0} Y_{L_x-\frac{1}{2},k_0+\frac{1}{2}} Z_{L_x,k_0} = -1$ has a strong non-invertible symmetry $D^{(1)}$.

3. Other choices of interface cuts between $\rho_{1\text{D-DASPT}}$ and $\rho_{\text{blue}^{k_0:k_1}}$

a. Interface cut at (l, k_0) and (L_x, k_0)

Let us consider an interface cut passing through (l, k_0) and (L_x, k_0) . The interface state is

$$\rho_{1\text{D-DASPT|blue}^{k_0:k_1}}^{(1)} = \prod_{i=0}^{l-1} \frac{(1 + Z_{i,k_0} X_{i+\frac{1}{2},k_0+\frac{1}{2}} Z_{i+1,k_0})}{2} \prod_{i=l+1}^{L_x-2} \frac{(1 - Y_{i,k_0} X_{i+\frac{1}{2},k_0} Y_{i+1,k_0})}{2} \prod_i \frac{(1 + \prod_i X_{i,k_0})}{2^{L_x}}. \quad (\text{D9})$$

Now we apply the symmetries on this state

$$\prod_i X_{i,k_0} \rho_{1\text{D-DASPT|blue}^{k_0:k_1}}^{(1)} = \rho_{1\text{D-DASPT|blue}^{k_0:k_1}}^{(1)} \quad (\text{D10a})$$

$$\prod_i X_{i+\frac{1}{2},k_0+\frac{1}{2}} \rho_{1\text{D-DASPT|blue}^{k_0:k_1}}^{(1)} = Z_{l,k_0} X_{l+\frac{1}{2},k_0+\frac{1}{2}} Y_{l+1,k_0} \times Y_{L_x-1,k_0} X_{L_x-\frac{1}{2},k_0+\frac{1}{2}} Z_{L_x,k_0} \rho_{1\text{D-DASPT|blue}^{k_0:k_1}}^{(1)}. \quad (\text{D10b})$$

When we add the projectors $Z_{l,k_0} X_{l+\frac{1}{2},k_0+\frac{1}{2}} Y_{l+1,k_0} = \pm 1$, and $Y_{L_x-1,k_0} X_{L_x-\frac{1}{2},k_0+\frac{1}{2}} Z_{L_x,k_0} = \pm 1$ the interface state is symmetric under strong $\mathbb{Z}_2^{(r)} \times \mathbb{Z}_2^{(b)}$ symmetry implying that the two states $\rho_{\text{1D-DASPT}}$ and $\rho_{\text{blue}^{k_0:k_1}}$ are in the same phase w.r.t the strong $\mathbb{Z}_2^{(r)} \times \mathbb{Z}_2^{(b)}$. However, these two are distinguished by non-invertible symmetry $D^{(1)}$ since $\rho_{\text{1D-DASPT}}$ has strong $D^{(1)}$ while $\rho_{\text{blue}^{k_0:k_1}}$ is not symmetric under $D^{(1)}$.

b. *Interface cut at $(l + \frac{1}{2}, k_0 + \frac{1}{2})$ and (L_x, k_0)*

Now let us consider an interface cut passing through $(l + \frac{1}{2}, k_0 + \frac{1}{2})$ and (L_x, k_0) . The interface state is

$$\rho_{\text{1D-DASPT|blue}^{k_0:k_1}}^{(2)} = \prod_{i=1}^{l-1} \frac{(1 + Z_{i,k_0} X_{i+\frac{1}{2},k_0+\frac{1}{2}} Z_{i+1,k_0})}{2} \prod_{i=l+1}^{L_x-2} \frac{(1 - Y_{i,k_0} X_{i+\frac{1}{2},k_0} Y_{i+1,k_0})}{2} \frac{(1 + \prod_i X_{i,k_0})}{2^{L_x}}. \quad (\text{D11})$$

Now we apply the symmetries on this state

$$\prod_i X_{i,k_0} \rho_{\text{1D-DASPT|blue}^{k_0:k_1}}^{(2)} = \rho_{\text{1D-DASPT|blue}^{k_0:k_1}}^{(2)} \quad (\text{D12a})$$

$$\prod_i X_{i+\frac{1}{2},k_0+\frac{1}{2}} \rho_{\text{1D-DASPT|blue}^{k_0:k_1}}^{(2)} = Z_{l,k_0} X_{l+\frac{1}{2},k_0+\frac{1}{2}} Y_{l+1,k_0} \times Y_{L_x-1,k_0} X_{L_x-\frac{1}{2},k_0+\frac{1}{2}} Z_{L_x,k_0} \rho_{\text{1D-DASPT|blue}^{k_0:k_1}}^{(2)}. \quad (\text{D12b})$$

When we add the projectors $Z_{l,k_0} X_{l+\frac{1}{2},k_0+\frac{1}{2}} Y_{l+1,k_0} = \pm 1$, and $Y_{L_x-1,k_0} X_{L_x-\frac{1}{2},k_0+\frac{1}{2}} Z_{L_x,k_0} = \pm 1$ the interface state is symmetric under strong $\mathbb{Z}_2^{(r)} \times \mathbb{Z}_2^{(b)}$ symmetry implying that the two states $\rho_{\text{1D-DASPT}}$ and $\rho_{\text{blue}^{k_0:k_1}}$ are in the same phase w.r.t the strong $\mathbb{Z}_2^{(r)} \times \mathbb{Z}_2^{(b)}$.

E. Commutative diagram

Let us consider a pure 2D state ρ . Now consider the single site Pauli decoherence channel

$$\xi_i[\rho] = \frac{1}{2} (\rho + \mathfrak{X}_i \rho \mathfrak{X}_i), \quad \xi_{\mathcal{A}}[\rho] = \prod_{i \in \mathcal{A}} \xi_i[\rho], \quad (\text{E1})$$

where \mathcal{A} is a subset of the sites and \mathfrak{X}_i be any Pauli operator X, Y or Z . Now let us denote the trace operation on a subset of sites \mathcal{B} by $\text{Tr}_{\mathcal{B}}$. Then we have

$$\text{Tr}_{\mathcal{B}}(\xi_{\mathcal{A}}[\rho]) = \xi_{\mathcal{A} \cap \mathcal{B}^c}[\text{Tr}_{\mathcal{B}}(\rho)]. \quad (\text{E2})$$

This can be proven in the following steps

$$\begin{aligned} \text{Tr}_{\mathcal{B}}(\xi_{\mathcal{A}}[\rho]) &= \text{Tr}_{\mathcal{B}} \left(\sum_{\substack{\{i\}, \\ i_i \in \mathcal{A}}} \mathfrak{X}_{i_1} \dots \mathfrak{X}_{i_r} \rho \mathfrak{X}_{i_1} \dots \mathfrak{X}_{i_r} \right) \\ &= \sum_{\{s\}_{\mathcal{B}}} \langle \{s\}_{\mathcal{B}} | \sum_{\substack{\{i\}, \\ i_i \in \mathcal{A}}} \mathfrak{X}_{i_1} \dots \mathfrak{X}_{i_r} \rho \mathfrak{X}_{i_1} \dots \mathfrak{X}_{i_r} | \{s\}_{\mathcal{B}} \rangle \\ &= \sum_{\substack{\{i\}, \\ i_i \in \mathcal{A} \cap \mathcal{B}^c}} \mathfrak{X}_{i_1} \dots \mathfrak{X}_{i_s} \sum_{\{s\}_{\mathcal{B}}} \langle \{s\}_{\mathcal{B}} | \rho | \{s\}_{\mathcal{B}} \rangle \mathfrak{X}_{i_1} \dots \mathfrak{X}_{i_s} \\ &= \xi_{\mathcal{A} \cap \mathcal{B}^c}[\text{Tr}_{\mathcal{B}}(\rho)]. \end{aligned} \quad (\text{E3})$$

In the second equality, we sum over the states in the basis of \mathfrak{X}_i operators at each site.

The above derivation then implies the following commutative diagram

$$\begin{array}{ccc} \rho_{\text{2D-pure}} & \xrightarrow{\text{Tr}_{\mathcal{B}}} & \rho_{\text{1D-mixed}} \\ \xi[\rho_{\text{2D-pure}}] \downarrow & & \downarrow \xi[\rho_{\text{1D-mixed}}] \\ \rho_{\text{2D-mixed}} & \xrightarrow{\text{Tr}_{\mathcal{B}}} & \rho'_{\text{1D-mixed}} \end{array}. \quad (\text{E4})$$

F. Some examples of 1D mixed state phases via decohering pure states (with \mathbb{Z}_2 degrees of freedom)

Here, we give examples of 1D mixed state by decohering the corresponding 1D pure state. The resulting mixed states in various cases below are related to the examples described in the main text and previous Appendices, where one traces over the bulk of 2D pure states. This corresponds to the top layer in the commutative diagram below. On the left end, we have the 2D pure state that we trace over to produce the 1D mixed state in the middle. The same mixed state can be obtained by decohering the 1D pure state in the right end.

$$\begin{array}{ccccc}
 \rho_{2\text{D-pure}} & \xrightarrow{\text{Tr}_B} & \rho_{1\text{D-mixed}} & \xleftarrow{\xi'[\rho_{1\text{D-pure}}]} & \rho_{1\text{D-pure}} \\
 \downarrow \xi[\rho_{2\text{D-pure}}] & & \downarrow \xi[\rho_{1\text{D-mixed}}] & \swarrow \xi \circ \xi'[\rho_{1\text{D-pure}}] & \\
 \rho_{2\text{D-mixed}} & \xrightarrow{\text{Tr}_B} & \rho'_{1\text{D-mixed}} & &
 \end{array} \tag{F1}$$

1. Example: 1D SWSSB by decohering the GHZ state

Consider the GHZ state with two symmetries. One is the 0-form \mathbb{Z}_2 symmetry, $\eta = \prod_i X_i$. The other one is a “1-form” symmetry $Z_i Z_j$, $i \neq j$. For periodic boundary condition, the density matrix is given by,

$$\rho_{GHZ} = \prod_i \frac{1 + Z_i Z_j}{2} \cdot \frac{1 + \eta}{2^N}, \tag{F2}$$

where N is the number of qubits of the system. Consider the local Kraus operators, $K_i = \{1, X_i\}$. The decohered density matrix is thus given by

$$\rho^{(1)} = \frac{1 + \eta}{2^N}. \tag{F3}$$

One can check this density matrix still has the strong η symmetry. However, the “1-form” $Z_i Z_j$ symmetry becomes weak.

$$Z_i Z_j \rho^{(1)} Z_i Z_j = \rho^{(1)}. \tag{F4}$$

Different extremal points are labeled by the charge of the strong symmetry. We have

$$\rho^{(2)} = Z_i \rho^{(1)} Z_j = \frac{1 - \eta}{2^N}. \tag{F5}$$

They can be distinguished by applying the strong symmetry operator,

$$\eta \rho^{(1)} = \rho^{(1)}, \quad \eta \rho^{(2)} = -\rho^{(2)}. \tag{F6}$$

The above two density matrices, $\rho^{(1)}$ and $\rho^{(2)}$, form a locally indistinguishable set, and further can be proved to be an information convex set. One can also check the Rényi-2 correlator of this state is non-vanishing. Therefore, this state is in the SWSSB phase.

We note that the form of $\rho^{(1)}$ appears in (16), where the mixed state $\rho_{\text{1D-DASPT}}^A$ was obtained by tracing over the bulk of the 2D cluster state. The act of tracing over the bulk there provides an effective decoherence channel on the boundary.

Additionally, both density matrices have weak Kramers-Wannier symmetry D , as in Eq. (25),

$$D \rho^{(1)} = \rho^{(1)} D, \quad D \rho^{(2)} = \rho^{(2)} D. \tag{F7}$$

If we instead decohere in $\{1, Z_i\}$ basis, then the resultant state is a mixture of $|0 \cdots 0\rangle$ and $|1 \cdots 1\rangle$. η becomes a weak symmetry and $Z_i Z_j$ is still a strong symmetry despite that its support is two, unlike that of the global symmetry η . However, now that η becomes a weak symmetry, and thus Z_i will no longer be regarded as a charge, as a weak symmetry does not have a conserved charge despite $\text{Tr}(\rho Z_i Z_j) = 1$, even for $|i - j| \rightarrow \infty$. One expects that a small perturbation will break the equal weight mixture, thereby breaking the weak symmetry η .

2. Example: 1D ASPT from decohering the cluster state in the Z basis

Consider the $\mathbb{Z}_2 \times \mathbb{Z}_2$ cluster state. In periodic boundary condition, the density matrix can be given as follows,

$$\rho_{\text{cl}} = \prod_{i \in e} \frac{1 + Z_{i-1}^o X_i^e Z_{i+1}^o}{2} \prod_{j \in o} \frac{1 + Z_{j-1}^e X_j^o Z_{j+1}^e}{2}. \quad (\text{F8})$$

Consider the local Kraus operators $K_{i \in e} = \{1, Z_i^e\}$. After decoherence, we get,

$$\rho'_{\text{cl}} = \prod_{j \in o} \frac{1 + Z_{j-1}^e X_j^o Z_{j+1}^e}{2}. \quad (\text{F9})$$

This density matrix has a weak 0-form symmetry $\eta^e = \prod_{i \in e} X_i^e$, and a strong 0-form symmetry $\eta^o = \prod_{i \in o} X_i^o$. One can calculate the expectation value of the strong string order parameter,

$$\text{Tr}(Z^e X^o X^o \dots X^o Z^e \rho'_{\text{cl}}) = 1. \quad (\text{F10})$$

It's straightforward to see the expectation value of the weak string order parameter is 1. In addition, one can also observe the weak symmetry localization,

$$X_i^e X_{i+1}^e \dots X_j^e \rho'_{\text{cl}} X_i^e X_{i+1}^e \dots X_j^e = Z_{i-1}^o Z_{j+1}^o \rho'_{\text{cl}} Z_{i-1}^o Z_{j+1}^o. \quad (\text{F11})$$

Therefore, this density matrix is in the averaged SPT (ASPT) phases [8, 9], classified by $H^2(\mathbb{Z}_2^s \times \mathbb{Z}_2^w, U(1))$. Equivalently, the state can be given by the domain wall decoration between the strong \mathbb{Z}_2^s symmetry and the weak \mathbb{Z}_2^w symmetry.

Additionally, the density matrix has a Kramers-Wannier symmetry $D^{(1)}$, as in Eq. (24),

$$D^{(1)} \rho'_{\text{cl}} = \rho'_{\text{cl}} D^{(1)}. \quad (\text{F12})$$

Comparing with the pure state case, which uses coherent proliferation of domain walls $\sum_{i \in \text{even}} Z_{i-1} X_i Z_{i+1}$ to obtain $Z_2 \otimes Z_2$ SPT, the mixed state case uses incoherent proliferation: using the channel $\sum_{i \in \text{even}} Z_{i-1} X_i Z_{i+1} [\]$, where $A[\rho] \equiv A \rho A^\dagger$.

3. Example: Coexistence of SWSSB and ASPT (i.e., DASPT) by decohering the cluster state in the X basis

Starting from the $\mathbb{Z}_2 \times \mathbb{Z}_2$ cluster state. Now we consider the Kraus operators to be $K_{i \in e} = \{1, X_i^e\}$. The decohered density matrix is given by

$$\rho_{\text{cl}}^{(1)} = \prod_{i \in e} \frac{1 + Z_{i-1}^o X_i^e Z_{i+1}^o}{2} \cdot \frac{1 + \eta^o}{2^N}. \quad (\text{F13})$$

Equivalently, the above density matrix can be obtained from tracing over the bulk of a 2d cluster state, as we studied in Sec. III B. One can notice that the first part of the density matrix resembles the density matrix of an ASPT phase, as we have shown in Eq. (F8), while the second part resembles an SWSSB phases, as we have shown in Eq. (F3). This coexistence of SWSSB and ASPT can also be understood as domain wall decoration between the all $|+\rangle$ state on the first layer and a SWSSB density matrix on the second.

The symmetries of this density matrix are given as follows: A strong 0-form symmetry η^e , a strong 0-form symmetry η^o , and a weak "1-form" symmetry $Z_i^o Z_j^o$. One can calculate the following properties,

$$Z^o X^e \dots X^e Z^o \rho_{\text{cl}}^{(1)} = \rho_{\text{cl}}^{(1)}, \quad (\text{F14a})$$

$$Z^e X^o \dots X^o Z^e \rho_{\text{cl}}^{(1)} Z^e X^o \dots X^o Z^e = \rho_{\text{cl}}^{(1)}, \quad (\text{F14b})$$

$$\frac{\text{Tr}(Z_i^o Z_j^o \rho_{\text{cl}}^{(1)} Z_i^o Z_j^o \rho_{\text{cl}}^{(1)})}{\text{Tr}((\rho_{\text{cl}}^{(1)})^2)} = 1. \quad (\text{F14c})$$

Different extremal points can be labeled by the charge of the η^o symmetry, and we obtain a second extremal point from the above state:

$$\rho_{\text{cl}}^{(2)} = Z_i^o \rho_{\text{cl}}^{(1)} Z_i^o = \rho_{\text{cl}}^{(1)} = \prod_{i \in e} \frac{1 + Z_{i-1}^o X_i^e Z_{i+1}^o}{2} \cdot \frac{1 - \eta^o}{2^N}. \quad (\text{F15})$$

$\rho_{\text{cl}}^{(1)}$ and $\rho_{\text{cl}}^{(2)}$ are locally indistinguishable due to the factor $1 \pm \eta^o$, and $\text{Tr}(\rho_{\text{cl}}^{(1)} \rho_{\text{cl}}^{(2)}) = 0$. Additionally, there is a KW symmetry,

$$D^{(1)} \rho_{\text{cl}}^{(1)} = \rho_{\text{cl}}^{(1)} D^{(1)}, \quad D^{(1)} \rho_{\text{cl}}^{(2)} = \rho_{\text{cl}}^{(2)} D^{(1)} \quad (\text{F16})$$

Therefore, this density matrix has both features of the ASPT phase and the SWSSB phase, and it was recently studied numerically in Ref. [65]. We note that the form of $\rho_{\text{cl}}^{(1)}$ is identical to (16), where the mixed state $\rho_{\text{1D-DASPT}}^{\text{A}}$ was obtained by tracing over the bulk of the 2D cluster state. The act of tracing over the bulk there provides an effective decoherence channel on the boundary.

In the open boundary condition case, the η^o symmetry is explicitly broken. Therefore, the SWSSB does not exist anymore. Instead, the ASPT phase can still survive, for which both strong and weak symmetry can be localized [9]. Therefore, one can still observe an ASPT phase in open boundary condition.

4. Example: Another DASPT by decohering the cluster state with nearest neighbor YY

Here, we still start with the 1D pure cluster state, whose density matrix is

$$\rho = \prod_{i \in o} \left(\frac{1 + Z_{i-1}^e X_i^o Z_{i+1}^e}{2} \right) \prod_{i \in e} \left(\frac{1 + Z_{i-1}^e X_i^e Z_{i+1}^o}{2} \right), \quad (\text{F17a})$$

which is identical to

$$\rho = \prod_{i \in e} \left(\frac{1 - Z_{i-2}^e Y_{i-1}^o X_i^e Y_{i+1}^o Z_{i+1}^e}{2} \right) \prod_{i \in o} \left(\frac{1 + Z_{i-1}^e X_i^o Z_{i+1}^e}{2} \right). \quad (\text{F17b})$$

But we now apply a different decoherence channel $\xi[\rho] = \prod_i \xi_i[\rho]$ where $\xi_i[\rho] = \frac{1}{2} (\rho + Y_i^o Y_{i+2}^o \rho Y_i^o Y_{i+2}^o)$. This yields

$$\rho_{\text{odd}}^{(1)} = \prod_{i \in e} \left(\frac{1 - Z_{i-2}^e Y_{i-1}^o X_i^e Y_{i+1}^o Z_{i+1}^e}{2} \right) \left(\frac{1 + \prod_{i \in o} X_i^o}{2^N} \right) \quad (\text{F18})$$

which can be seen identical to $\rho_{\text{blue}}^{\text{A}}$ in (32).

We mention yet another example that starting with pure state non-invertible SPT in (37), we applied a decoherence channel that consists of nearest-neighbor YY's to obtain the state in (36).

G. 1D examples of mixed state phases and non-invertible SWSSB

For the $\mathbb{Z}_2 \times \mathbb{Z}_2$ cluster state, consider the following Kraus operators, $K_i = \{1, X_i\}$ on both sublattices, as opposed to just one sublattice considered in Appendix F3. The decohered density matrix is given by

$$\rho^{(1)} = \frac{1 + \eta^e}{2^N} \frac{1 + \eta^o}{2^N}. \quad (\text{G1})$$

The symmetries of this density matrix are given as follows: A strong 0-form symmetry η^e , a strong 0-form symmetry η^o , a weak “1-form” symmetry $Z_i^e Z_j^e$, a weak “1-form” symmetry $Z_i^o Z_j^o$, and a Kramers-Wannier symmetry $D^{(1)}$.

This density matrix is in the SWSSB phase for $\mathbb{Z}_2 \times \mathbb{Z}_2$ symmetry. Different extremal points are labeled by the charges (also interconvertible by the charge operators). We have

$$\begin{aligned} \rho_{++} &= \frac{1 + \eta^e}{2^N} \frac{1 + \eta^o}{2^N}, & \rho_{+-} &= \frac{1 + \eta^e}{2^N} \frac{1 - \eta^o}{2^N}, \\ \rho_{-+} &= \frac{1 - \eta^e}{2^N} \frac{1 + \eta^o}{2^N}, & \rho_{--} &= \frac{1 - \eta^e}{2^N} \frac{1 - \eta^o}{2^N} \end{aligned} \quad (\text{G2})$$

The above matrices are locally indistinguishable, and orthogonal to each other. In this section, we rescale $D^{(1)} \rightarrow 2D^{(1)}$. The first density matrix only has weak $D^{(1)}$ symmetry, while the other three have strong $D^{(1)}$ symmetry with eigenvalue 0. To further get the $\text{Rep}(D_8)$ SWSSB density matrix, we need to symmetrize the first density matrix. We get,

$$\rho_{\text{KW}_1} = \frac{1 + \eta^e}{2^N} \frac{1 + \eta^o}{2^N} + \frac{2D^{(1)}}{4^N}. \quad (\text{G3})$$

One can show that

$$D^{(1)}\rho_{KW_1} = 2\rho_{KW_1}. \quad (G4)$$

Here we use the following facts:

$$D^{(1)}\eta_e = \eta_e D^{(1)} = D^{(1)}, \quad D^{(1)}\eta_o = \eta_o D^{(1)} = D^{(1)}, \quad (D^{(1)})^2 = 1 + \eta_e + \eta_o + \eta_e\eta_o. \quad (G5)$$

The other density matrix that carries nontrivial $D^{(1)}$ charge is given by

$$\rho_{KW} = \frac{1 + \eta^e}{2^N} \frac{1 + \eta^o}{2^N} - \frac{2D^{(1)}}{4^N}. \quad (G6)$$

One can show that

$$D^{(1)}\rho_{KW_2} = -2\rho_{KW_2}. \quad (G7)$$

Similar study for the $\text{Rep}(G)$ SWSSB on the qudit system can be found in Ref. [33, 39]. $\text{Rep}(D_8)$ SWSSB are labeled by the charge of the $\text{Rep}(D_8)$ symmetry, which are classified by the following homomorphism,

$$[\omega] \in \text{Hom}(\text{Rep}(D_8), \mathbb{C}), \quad (G8)$$

where $[\omega]$ represents different equivalent classes. We show these classes in Table. G.

	η^e	η^o	$D^{(1)}$
ρ_{KW_1}	1	1	2
ρ_{+-}	1	-1	0
ρ_{-+}	-1	1	0
ρ_{--}	-1	-1	0
ρ_{KW_2}	1	1	-2

Our goal is to calculate $\text{Tr}(D^{(1)})$, which is the same as $\text{Tr}(\mathbb{V}D^{(1)}\mathbb{V})$, where $\mathbb{V}D^{(1)}\mathbb{V}$ is the Kennedy-Tasaki transformation that can be written in terms of an MPO [74].

Now, consider the $2N$ spins with two spins per unit cell. Let us consider this effective site that contains two spins. The MPO tensor at the j^{th} site is

$$u^j = \begin{pmatrix} |++\rangle_j \langle ++| + |+-\rangle_j \langle +-| & |-\rangle_j \langle -+| - |--\rangle_j \langle --| \\ |-\rangle_j \langle -+| + |--\rangle_j \langle --| & |++\rangle_j \langle ++| - |+-\rangle_j \langle +-| \end{pmatrix}. \quad (G9)$$

The matrix is in the virtual space while the matrix element which is an operator is acting on the physical space. Then, we have

$$\mathbb{V}D^{(1)}\mathbb{V} = \text{Tr}_{\mathcal{H}_{\text{virt}}} (u^N u^{N-1} \dots u^1), \quad (G10)$$

where the trace is over the virtual space. We can explicitly evaluate the trace over the physical space of the operator $\mathbb{V}D^{(1)}\mathbb{V}$

$$\begin{aligned} \text{Tr}_{\mathcal{H}_{\text{phy}}} (\mathbb{V}D^{(1)}\mathbb{V}) &= \text{Tr}_{\mathcal{H}_{\text{phy}}} (\text{Tr}_{\mathcal{H}_{\text{virt}}} (u^N u^{N-1} \dots u^1)) \\ &= \text{Tr}_{\mathcal{H}_{\text{virt}}} (\text{Tr}_{\mathcal{H}_{\text{phy}}} (u^N u^{N-1} \dots u^1)) \\ &= \text{Tr}_{\mathcal{H}_{\text{virt}}} (\text{Tr}(u^N) \text{Tr}(u^{N-1}) \dots \text{Tr}(u^1)) \\ &= \text{Tr}_{\mathcal{H}_{\text{virt}}} \left(\begin{pmatrix} 2 & 0 \\ 2 & 0 \end{pmatrix}^N \right) \\ &= \text{Tr}_{\mathcal{H}_{\text{virt}}} \left(\begin{pmatrix} 2^N & 0 \\ 2^N & 0 \end{pmatrix} \right) \\ &= 2^N. \end{aligned} \quad (G11)$$

Since $V^2 = 1$, $\text{Tr}_{\mathcal{H}_{\text{phy}}}(\text{VD}^{(1)}V) = \text{Tr}_{\mathcal{H}_{\text{phy}}}(D^{(1)}) = 2^N$.

Therefore, we have,

$$\lim_{N \rightarrow \infty} \text{Tr}(\rho_{\text{KW}_1}) = \lim_{N \rightarrow \infty} \text{Tr}(\rho_{\text{KW}_2}) = 1. \quad (\text{G12})$$

In the thermodynamics limit $N \rightarrow \infty$, the above five density matrices are locally indistinguishable, and they are orthogonal to each other. Therefore, they define the five extremal points of the information convex set for the $\text{Rep}(D_8)$ SWSSB.

The above MPO analysis implies that the properly normalized duality operator $D^{(1)}$ has zero trace in the thermodynamic limit. In general, the computation of this trace requires careful regularization. In cases where we have a TQFT with degenerate vacua, for example at the end of a certain RG flow preserving categorical symmetry, trace of a topological operator vanishes if the corresponding defect Hilbert space is empty [75]. In 2D rational CFTs such as the Ising CFT and the tricritical Ising CFT, the trace of the duality operator vanishes when restricted to the primary states of the theory quantized on a circle.

H. 1D $\mathbb{Z}_3^{(s)} \times \mathbb{Z}_3^{(w)}$ ASPT: two ASPTs and the interface between them

1. ASPTs from decohering pure state SPTs

In this section, we consider the $\mathbb{Z}_3 \times \mathbb{Z}_3$ cluster state and consider various decoherence channel. According to the classification of bosonic SPTs, in 1D $\mathbb{Z}_3 \times \mathbb{Z}_3$ symmetric SPTs are classified by $H^2(\mathbb{Z}_3 \times \mathbb{Z}_3, U(1)) = \mathbb{Z}_3$. So there are two non-trivial SPTs. We consider one of them, concretely

$$\rho_{\text{SPT}_1} = \prod_{i \in e} \left(\frac{1 + Z_{i-1}^{\dagger} X_i^e Z_{i+1}^o + Z_{i-1}^o X_i^{\dagger} Z_{i+1}^{\dagger}}{3} \right) \times \prod_{j \in o} \left(\frac{1 + Z_{j-1}^e X_j^o Z_{j+1}^{\dagger} + Z_{j-1}^{\dagger} X_j^{\dagger} Z_{j+1}^e}{3} \right). \quad (\text{H1})$$

This state can be equivalently written as

$$\prod_{i \in o} CZ_{i,i-1} CZ_{i,i+1}^{\dagger} |+\rangle^{\otimes \Delta_e} |+\rangle^{\otimes \Delta_o}, \quad \text{with } |+\rangle = \frac{(|0\rangle + |1\rangle + |2\rangle)}{3}, \quad \text{and } CZ_{i,i+1} = \sum_{a,b=0}^2 \omega^{ab} |a,b\rangle \langle a,b|.$$

Now consider the local Kraus operators $K_{i \in e} = \{1, Z_i^e, Z_i^{\dagger}\}$. After decoherence, we get the mixed state

$$\rho_{\text{m-SPT}_1} = \prod_{j \in o} \left(\frac{1 + Z_{j-1}^e X_j^o Z_{j+1}^{\dagger} + Z_{j-1}^{\dagger} X_j^{\dagger} Z_{j+1}^e}{3} \right). \quad (\text{H2})$$

This density matrix has strong 0-form symmetry $\eta^o = \prod_{j \in o} X_j^o$ and weak 0-form symmetry $\eta^e = \prod_{j \in e} X_j^e$. One can calculate the expectation value of the strong string order parameter,

$$\text{Tr}(Z^e X^o X^o \dots X^o Z^{\dagger} \rho_{\text{m-SPT}_1}) = 1. \quad (\text{H3})$$

One can also calculate the expectation value of the weak string order parameter on the other sublattice,

$$\text{Tr}(Z^{\dagger} X^e X^e \dots X^e Z^o \rho_{\text{m-SPT}_1} Z^o X^{\dagger} X^{\dagger} \dots X^{\dagger} Z^{\dagger}) = 1. \quad (\text{H4})$$

Now let us consider the other non-trivial SPT

$$\rho_{\text{SPT}_2} = \prod_{i \in e} \left(\frac{1 + Z_{i-1}^o X_i^e Z_{i+1}^{\dagger} + Z_{i-1}^{\dagger} X_i^{\dagger} Z_{i+1}^o}{3} \right) \times \prod_{j \in o} \left(\frac{1 + Z_{j-1}^{\dagger} X_j^o Z_{j+1}^e + Z_{j-1}^e X_j^{\dagger} Z_{j+1}^{\dagger}}{3} \right). \quad (\text{H5})$$

This state can be equivalently written as

$$\prod_{i \in o} CZ_{i,i-1}^{\dagger} CZ_{i,i+1} |+\rangle^{\otimes \Delta_e} |+\rangle^{\otimes \Delta_o}, \quad \text{with } |+\rangle = \frac{(|0\rangle + |1\rangle + |2\rangle)}{3}, \quad \text{and } CZ_{i,i+1} = \sum_{a,b=0}^2 \omega^{ab} |a,b\rangle \langle a,b|.$$

Now consider the local Kraus operators $K_{i \in e} = \{1, Z_i^e, Z_i^{e\dagger}\}$. After decoherence, we get the mixed state

$$\rho_{\text{m-SPT}_2} = \prod_{j \in o} \left(\frac{1 + Z_{j-1}^{e\dagger} X_j^o Z_{j+1}^e + Z_{j-1}^e X_j^{o\dagger} Z_{j+1}^{e\dagger}}{3} \right). \quad (\text{H6})$$

This density matrix has strong 0-form symmetry $\eta^o = \prod_{j \in o} X_j^o$ and weak 0-form symmetry $\eta^e = \prod_{j \in e} X_j^e$. One can calculate the expectation value of the strong string order parameter,

$$\text{Tr} (Z^{e\dagger} X^o X^o \dots X^o Z^e \rho_{\text{m-SPT}_2}) = 1. \quad (\text{H7})$$

One can also calculate the expectation value of the weak string order parameter on the other sublattice,

$$\text{Tr} (Z^o X^e X^e \dots X^e Z^{o\dagger} \rho_{\text{m-SPT}_2} Z^{o\dagger} X^{e\dagger} X^{e\dagger} \dots X^{e\dagger} Z^o) = 1. \quad (\text{H8})$$

2. Interface between the two $\mathbb{Z}_3^{(s)} \times \mathbb{Z}_3^{(w)}$ ASPTs

According to the classification of mSPTs [8], $H^1(\mathbb{Z}_3, H^1(\mathbb{Z}_3, U(1)))$, there are three mSPTs with \mathbb{Z}_3 strong and \mathbb{Z}_3 weak symmetry. One of the SPTs is the trivial SPT. To write down the other two non-trivial SPTs, we consider N sites on a ring. We label them odd o and even e . Let X and Z be \mathbb{Z}_3 shift and clock operators. The two non-trivial SPTs are

$$\rho_{\text{m-SPT}_1} = \prod_{j \in o} \left(\frac{1 + Z_{j-1}^e X_j^o Z_{j+1}^{e\dagger} + Z_{j-1}^{e\dagger} X_j^{o\dagger} Z_{j+1}^e}{3} \right) \quad (\text{H9a})$$

$$\rho_{\text{m-SPT}_2} = \prod_{j \in o} \left(\frac{1 + Z_{j-1}^{e\dagger} X_j^o Z_{j+1}^e + Z_{j-1}^e X_j^{o\dagger} Z_{j+1}^{e\dagger}}{3} \right). \quad (\text{H9b})$$

Now let us consider an interface between the two mSPTs: $\rho_{\text{m-SPT}_1}$ and $\rho_{\text{m-SPT}_2}$, where the two interfaces are put at l and $2N - 1$. Then the mixed state with this interface is

$$\rho_{\text{m-SPT}_1|\text{m-SPT}_2} = \prod_{\substack{1 \leq j < l \\ j \in o}} \left(\frac{1 + Z_{j-1}^e X_j^o Z_{j+1}^{e\dagger} + Z_{j-1}^{e\dagger} X_j^{o\dagger} Z_{j+1}^e}{3} \right) \prod_{\substack{l < j \leq 2N-1 \\ j \in o}} \left(\frac{1 + Z_{j-1}^{e\dagger} X_j^o Z_{j+1}^e + Z_{j-1}^e X_j^{o\dagger} Z_{j+1}^{e\dagger}}{3} \right). \quad (\text{H10})$$

On this mixed state, we act with the strong symmetry and its action localizes at the two interfaces

$$\prod_{j \in o} X_j^o \rho_{\text{m-SPT}_1|\text{m-SPT}_2} = Z_{l-1}^e X_l^o Z_{l+1}^e Z_{2N-2}^{e\dagger} X_{2N-1}^o Z_{2N}^{e\dagger} \rho_{\text{m-SPT}_1|\text{m-SPT}_2} \equiv \mathbb{X}_l \mathbb{X}_{2N-1} \rho_{\text{m-SPT}_1|\text{m-SPT}_2}. \quad (\text{H11})$$

In particular, \mathbb{X}_l and \mathbb{X}_{2N-1} are charged under the weak symmetry $\prod_{j \in e} X_j^e$. This implies that, if we add the projection onto $\mathbb{X}_l = \pm 1$ and $\mathbb{X}_{2N-1} = \pm 1$ to the interface state $\rho_{\text{m-SPT}_1|\text{m-SPT}_2}$ to preserve the strong symmetry $\prod_{j \in o} X_j^o$, we explicitly break the weak symmetry to nothing.